ACTA ENTOMOLOGICA
MUSEI NATIONALIS PRAGAE
ISSN 1804-6487 (online) – 0374-1036 (print)
2024
64(1): 47–66
doi: 10.37520/aemnp.2024.005
www.aemnp.eu

RESEARCH PAPER

Myrmeleon shalulianus sp. nov. (Neuroptera: Myrmeleontidae), and the first record of *Taiwanon* bee fly (Diptera: Bombyliidae) on *Myrmeleon trigonois* in China

Yuchen ZHENG[1)], Xuankun LI[1)], Gang YAO[2)] & Xingyue LIU[1,*)]

[1)] Department of Entomology, China Agricultural University, Beijing 100193, China; e-mails: zhengyuchenantlion@gmail.com; xuankun.li@cau.edu.cn; xingyue_liu@yahoo.com
[2)] Jinhua Polytechnic, Jinhua, Zhejiang 321007, China; e-mail: 538435@qq.com
*) corresponding author

Accepted:
27th April 2024

Published online:
30th May 2024

Abstract. The antlion species *Myrmeleon trigonois* Bao & Wang, 2006 is endemic to Chinese mainland; it has pronotum with a pair of pale yellow spots, and modified ectoproct, forming a hook-like projection posteroventrally. Based on morphological comparison and molecular evidence, we found that all paratypes of *M. trigonois* represent a different species than its holotype. Here, *Myrmeleon shalulianus* Zheng & Liu, sp. nov., is described to accommodate all paratypes of *M. trigonois* and a series of newly supplemented specimens from Yunnan (China). The distribution pattern of these two species is clarified. Larvae of both *M. trigonois* and *M. shalulianus* sp. nov. are described and compared. Furthermore, the bee fly parasitoid (Diptera: Bombyliidae) of the genus *Taiwanon* Evenhuis, 2018 was reared from the immature stages of *M. trigonois* in an artificial environment. *Taiwanon* is newly recorded from the Chinese mainland.

Key words. Neuroptera, Myrmeleontoidea, Myrmeleontidae, Myrmeleontini, Diptera, Bombylidae, Anthracinae, DNA barcoding, larval description, new species, parasitoid, China, Oriental Region

Zoobank: https://zoobank.org/urn:lsid:zoobank.org:pub:AED32036-DC9D-445E-AA7D-C213DEBC27E8

Introduction

Myrmeleontidae (antlions and owlflies) is the most species-rich lacewing family, comprising ca. 2100 species in 304 genera (Machado et al. 2019, Oswald 2023) at present. The type genus, *Myrmeleon* Linnaeus, 1767, is cosmopolitan with more than 190 known species, which is among the most diverse within the family (Badano et al. 2016, Wang et al. 2018, Machado et al. 2019, Michel & Akoudjin 2023, Oswald 2023). The adults of most species of *Myrmeleon* can be characterized by plain hyaline wings; the forewing RP origin distad of MP and CuA bifurcated, 2A running close to 1A for a short distance and bending at a sharp angle toward 3A, crossveins on the costal space mostly not interconnected by oblique vein; the hindwing with at least four presectoral crossveins; hind tarsomere 1 shorter than hind tarsomere 5; male gonocoxites 11 usually round-arched; the female anterior branches of gonocoxites 8 tuberculated while the posterior branches slender digitiform; and gonocoxites 9 and ventral ectoproct with stout and blunt setae. *Myrmeleon* larvae are well known for creating pit-form traps in the sand and fine soil to ambush their prey (Badano & Pantaleoni 2014). It makes this genus a dominant group of antlions, and consequently cosmopolitan in distribution, as the building of pit-shaped traps makes predation more efficient (Mansell 1999, Klokočovnik & Devetak 2022). Although the trap building behavior is common and specific to Myrmeleontinae (e.g., Myrmeleontini, Myrmecaelurini, Nesoleontini, and some Brachynemurini), the method of building traps varies in different clades (Devetak et al. 2013, Badano & Pantaleoni 2014). Phylogenetically, the monophyly of *Myrmeleon* has never been tested/revised (Badano et al. 2017a, Michel et al. 2017, Machado et al. 2019) and it contains 26 synonyms (Stange 2004). In addition, due

to lack of morphological characters of *Myrmeleon* adults, distinguishing closely related species is challenging, and the cases of overly delicate or rough classification within *Myrmeleon* cause another difficulty in revising this genus.

Bee flies (Diptera: Bombyliidae) are the only known dipteran group including parasitoids of immature stages of antlions (Nartshuk et al. 2019). Nine genera of bee flies have been recorded to use antlions as hosts, all belonging to the same subfamily Anthracinae (Nartshuk et al. 2019), but spanning four out of the seven tribes: Anthracini (*Anthrax* Scopoli, 1763), Exoprosopini (*Micomitra* Bowden, 1964 and *Pterobates* Bezzi, 1921), Villini (*Villa* Lioy, 1864, *Chrysanthrax* Osten Sacken, 1886, *Dipalta* Osten Sacken, 1877, and *Paravilla* Painter, 1933), and Villoestrini (*Oestranthrax* Bezzi, 1921 and *Taiwanon* Evenhuis, 2018). The bee fly genus *Taiwanon* is a monotypic genus first described from Taiwan, China. The type species, *Taiwanon phormae* Evenhuis, 2018, was reared from *Dendroleon esbenpeterseni* Miller & Stange, 1999, an antlion species whose immatures do not make pits (Evenhuis 2018, Nartshuk et al. 2019).

Nineteen species of *Myrmeleon* have been recorded from China (Ábrahám 2017, Wang et al. 2018, Yang et al. 2018, Hassan et al. 2022), among which *M. trigonois* Bao & Wang, 2006 is endemic to Chinese mainland (Bao & Wang 2006). Based on the type specimens (Fig. 2) and newly supplemented specimens, we found that all paratypes of *M. trigonois* represent a different species than its holotype. Therefore, a new species, *Myrmeleon shalulianus* Zheng & Liu sp. nov., is described. It is endemic to the mid-elevation dry-hot river valley of the Jinshajiang River in Shaluli mountain range (Sichuan to Yunnan) (Fig. 1). Larvae of both *M. trigonois* and *M. shalulianus* sp. nov. are described and compared. Furthermore, the bee fly parasitoid (Diptera: Bombyliidae) of the genus *Taiwanon* Evenhuis, 2018 was reared from the immature stages of *M. trigonois* in an artificial environment. This genus is newly recorded from mainland China (Figs 10–12).

Material and methods

Genitalia were prepared by clearing the apex of the abdomen with 20% KOH at 135°C for seven minutes. After rinsing the KOH with distilled water, the apex of the abdomen was transferred to glycerin for further examination. Habitus photos were taken using a Nikon® D850 digital camera with an AF-S Micro Nikkor 105 mm 1/2.8G ED lens. The head, thorax, and legs were photographed by a Nikon® D850 digital camera with a Laowa® 25mm F/2.8 2.5–5.0X Ultra Macro lens. The photos of pretarsal claws and genitalia were taken using a Leica® DM2000 fitted with a Nikon® D850 digital camera.

Larval specimens were preserved in 95% alcohol under -24°C, while the remaining larvae were reared to obtain adults for identification and bee-fly parasites. All living larvae were placed separately into 200 ml paper cups two-thirds full of sand, which allowed them to create pit-shaped traps as they would in their natural environment. A stick made from a paper napkin was put in each cup so that after emergence, the adult could climb upward. Rearing was carried out at room temperature (16–27°C). The antlion larvae were fed with the workers of termites, *Reticulitermes speratus* (Kolbe, 1885) (Blattodea: Termitidae), and the Turkestan cockroach, *Blatta lateralis* (Walker, 1868) (Blattodea: Blattidae).

The classification system of Myrmeleontidae follows Machado et al. (2019). Terminology of wing venation mainly follows Breitkreutz et al. (2017), while that of wing fields follows Machado & Oswald (2020). Terminology of genitalia mainly follows Aspöck & Aspöck (2008), Badano et al. (2017b,c) and Zheng et al. (2022, 2023). Terminology of the antlion larval morphology follows Badano & Pantaleoni (2014).

Abbreviations for Myrmeleontidae:

A	anal veins;
agx8	anterior branches of gonocoxites 8;
agx9	anterior gonocoxites 9;
BL	Banksian line;
C	costa;
CuA	cubitus anterior;
CuP	cubitus posterior;
Ds	digging setae;
ect	ectoprocts;
gp	gonapophyses;
gst	gonostylus;
gx	gonocoxites;
MA	media anterior;
MP	media posterior;
Ms	mesothoracic spiracles;
pgx8	posterior branches of gonocoxites 8;
pgx9	posterior gonocoxites 9;
pp	pregenital plate;
RA	radius anterior;
RP	radius posterior;
S	sternum;
Sc	subcosta;
1t	first tooth;
2t	second tooth;
3t	third tooth.

Abbreviations for Bombyliidae:

aap	anterior antennal process;
absr	abdominal spiracle;
dpp	dorsal posterolateral process;
fsp	frontal spine;
lesh 1	fore leg sheath;
lesh 2	middle leg sheath;
lesh 3	hind leg sheath;
lfsp	lateral facial spine;
lsh	labral sheath;
mfha	median facial hair;
msh	maxillary sheath;
pap	posterior antennal process;
pash	palpal sheath;
plfha	posterolateral facial hair;
pmc	posterior mesothoracic callosity;
prsh	proboscidal sheath;
vpp	ventral posterolateral process;
wsh	wing sheath.

To facilitate species identification, we sequenced the barcode region of the cytochrome C oxidase subunit 1 (COI) gene of the specimens of *Myrmeleon*. The total genomic DNA of the samples from CAU was extracted from the mesothoracic muscle of adults or larvae by using the TIANamp Micro DNA Kit (TIANGEN®, Beijing, China). The COI barcodes were amplified using the primers COI-

1-R (5'-TAAACTTCTGGATGT-CCAAAAAATCA-3') and COI4-F (5'-TGTAAAACGACG-GCCAGTAAACTA-ATARCCTTCAAAG-3') (Park et al. 2010, Lai et al. 2021). The thermal cycling program consisted of the initial denaturation at 95°C for 5 min, followed by 39 cycles of 95°C denaturation for 10 s, 52°C annealing for 50 s, 65°C extension for 1 min, and the final extension at 65°C for 10 min. PCR products were sequenced bidirectionally by the PCR-based method in Sangon Biotech (Shanghai).

Genetic distances of the COI barcode region (663 bp)

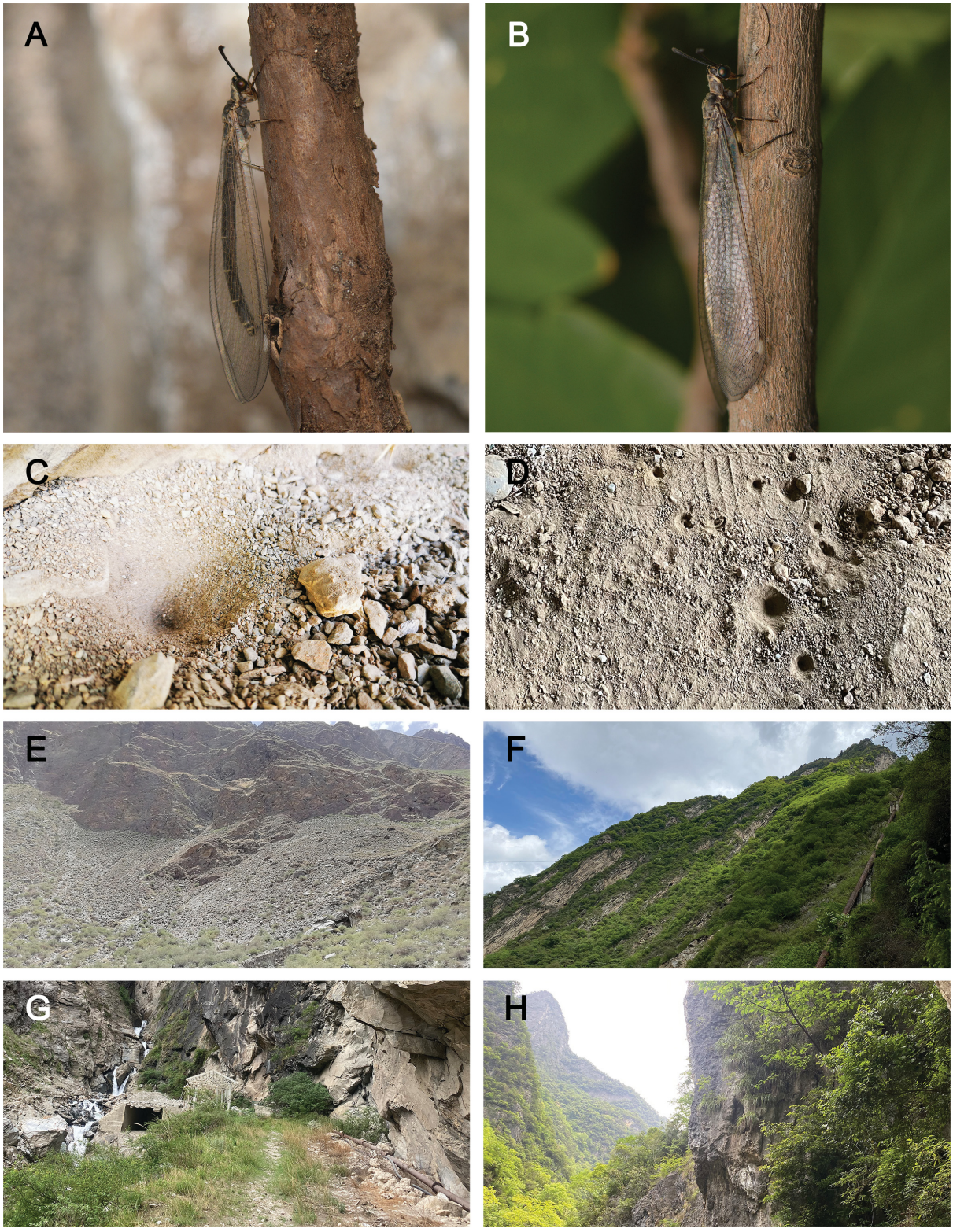

Fig. 1. A – living adult of *Myrmeleon shalulianus* Zheng & Liu sp. nov., female, Hutiaoxia, Yunnan, type locality (photo by Yuchen Zheng); B – living adult of *M. trigonois* Bao & Wang, 2006, female, Wenchuan, Sichuan (photo by Yuchen Zheng); C – pit-form trap of *M. shalulianus* sp. nov., Batang, Sichuan (photo by Di Li); D – pit-form traps of *M. trigonois*, Guangyuan, Sichuan (photo by Wenkai Kou); E, G – habitats of *M. shalulianus* sp. nov., E – Batang, Sichuan (photo by Di Li), G – Hutiaoxia, Yunnan, type locality (photo by Yuchen Zheng); F, H – habitats of *M. trigonois*, F – Wenchuan, Sichuan, H – Lanying, Chongqing (photos by Yuchen Zheng).

were calculated using MEGA 6.0 (Tamura et al. 2013) with the Kimura 2 Parameter (K2P) model (Kimura 1980). The phylogenetic study included the following three analyses: Maximum likelihood (ML) analysis was performed with IQ-TREE (Nguyen et al. 2015); Bayesian inference analysis was carried out with MrBayes 3.2.7a as implemented on the CIPRES Portal (Miller et al. 2010); Neighbour-joining (NJ) approach was performed in MEGA 6.0. The DNA sequences of the COI barcode region of the present samples are deposited in GenBank. The accession numbers of the data used in this paper can be found in Table 1.

All specimens herein examined are deposited in the Entomological Museum, China Agricultural University (CAU), Beijing, China.

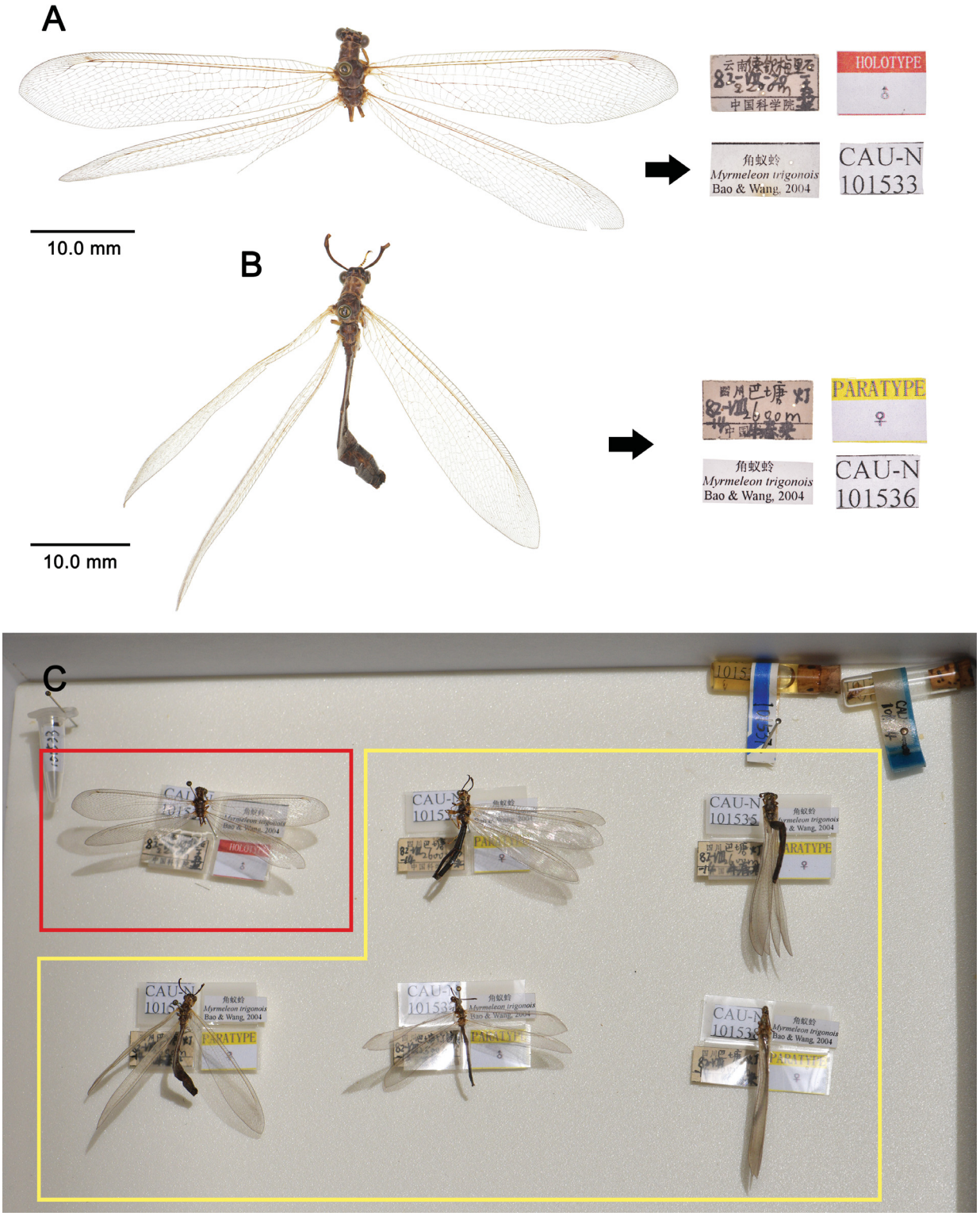

Fig. 2. Types of *Myrmeleon trigonois* Bao & Wang, 2006 based on Bao & Wang (2006). A – holotype, male; B – one of paratypes, treated as *M. shalulianus* Zheng & Liu sp. nov.; C – photos of all type specimens of *M. trigonois*, red box indicates the holotype, yellow box indicates all paratypes treated here as *M. shalulianus* sp. nov.

Results

Order Neuroptera Linnaeus, 1758

Genus *Myrmeleon* Linnaeus, 1767

Myrmeleon Linnaeus, 1767: 913. Type species: *Myrmeleon formicarium* Linnaeus, subsequent designation by Latreille (1810: 435). For details of synonyms, see Stange (2004).

Myrmeleon shalulianus Zheng & Liu sp. nov.

Chinese common name: 沙鲁里蚁蛉

(Figs 1A, C; 2B–C; 3A–B; 4; 5; 8A, C, E, G; 9A–B, E, G; 13; 14)

Type material. Holotype: ♂ (reared to adult, emerged in 13.viii.2023), CHINA: Yunnan, Diqing, Shangri-la, Hutiaoxia Town [虎跳峡镇], Bendiwan [本地湾], 2200 m, 4.vii.2023, Yuchen Zheng (CAU). Paratypes: 12 ♂♂ 23 ♀♀ and 32 larvae: 1 ♀ (reared to adult, emerged in 14.viii.2023), same information as holotype (CAU); 4 ♂♂, CHINA: Yunnan, Diqing, Shangri-la, Hutiaoxia Town, Jiangbian Village [江边村], Zanba [咱八], 2000–2100 m, 3.vii.2023, Yuchen Zheng (CAU); 1 ♂, CHINA: Yunnan, Lijiang, Yulong County [玉龙县], Daju Township [大具乡], 2100 m, 8.viii.2020, Haolin Gan (CAU); 2 ♀♀, CHINA: Sichuan, Garze, Baiyu County [白玉县], Gaiyu Township [盖玉乡], 2759 m, 24.vii.2023, Hao Xun (CAU); 4 ♂♂ 8 ♀♀, CHINA: Sichuan, Garze, Batang County [巴塘县], Suwalong Township [苏哇龙乡], Suwalong Village, 2409 m, 1–4.vii.2020, Di Li & Yuezheng Tu (CAU); 2 ♀♀, CHINA: Sichuan, Garze, Batang County, Changbo Township [昌波乡], Ruiwa Village [锐哇村], 2468 m, 6.vii.2019, Di Li (CAU); 3 ♀♀, CHINA: Sichuan, Garze, Batang, 2600 m, 14.viii.1982, Chunlai Niu (original paratypes of *Myrmeleon trigonois* Bao & Wang, 2006) (CAU); 1 ♂ 1 ♀, CHINA: Sichuan, Garze, Batang, 2500–2600 m, 13–14.viii.1982, Shuyong Wang (original paratypes of *Myrmeleon trigonois* Bao & Wang, 2006) (CAU); 2 ♂♂ 5 ♀♀, CHINA: Sichuan, Garze, Derong County [得荣县], Guxue Township [古学乡], Xiayong Village [下拥村], 2088 m, 7–9.vii.2020, Yuezheng Tu & Di Li (CAU); 1 ♀, CHINA: Sichuan, Liangshan, Muli County [木里县], Mairi Township [麦日乡], 2662 m, 25.vii.2023, Hao Xun (CAU); Larvae: 2 larvae of 2nd instar and 30 larvae of 3rd instar, same information as holotype (CAU).

Diagnosis. ***Adult.*** Gena mostly pale yellow, anteriorly dark brown (Fig. 4B). Pale yellowish part of the lateral margin of pronotum wide. Mesoscutellum laterally with a pair of pale yellowish spots. Hind femur dorsally yellow (Fig. 4A). Tarsomeres generally yellow, and dark brown distally (Figs 4A, 8C). Wing veins pale yellow, yellowish-brown and dark brown; Sc generally with alternating pale yellow and dark brown in basal half, fully pale yellow in distal half; R fully yellowish-brown; marginal veins dark brown (Figs 2B–C, 3A–B, 4A, 8A). Abdominal terga 3–8 each medially with a slender longitudinal yellowish-brown stripe (Figs 3A–B, 4A, 8E). Male anterior gonocoxites 9 slender, forming a V-shaped structure in ventral view, posterior gonocoxites 9 small, coniform; gonocoxites 11 slender round-arched (Figs 4H–L, 8G).

Larva. Head anteromedially with a pair of large subtriangular dark brown markings in ventral view (Figs 5B, 9B).

Description. ***Adult.*** *Size*. Head width: 2.64–3.14 mm; forewing length: 27.53–32.16 mm; hindwing length: 26.95–30.76 mm.

Head. Vertex raised, black, anteriorly with brown annular marking, laterally with pair of brown markings. Scape dorsally brown, ventrally black; pedicel and flagellum black (Fig. 4C). Gena wide, mostly pale yellow, anteriorly dark brown (Fig. 4B). Frons mostly black. Clypeus black, margin yellowish-brown (Fig. 4B). Labrum

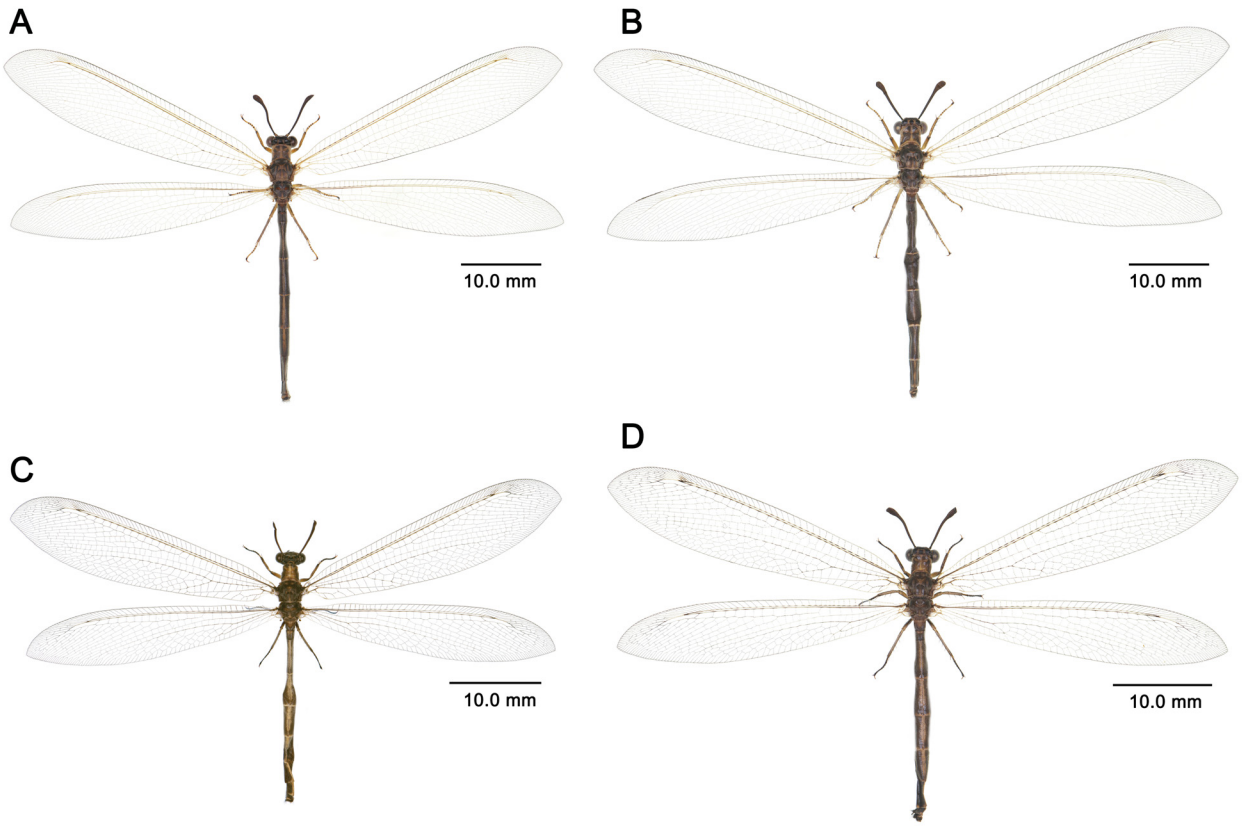

Fig. 3. Habitus of adults. A–B – *Myrmeleon shalulianus* Zheng & Liu sp. nov.: A – male, holotype; B – female, holotype, Hutiaoxia, Yunnan, type locality. C–D – *M. trigonois* Bao & Wang, 2006: C – male, Danba, Sichuan; D – female, Lixian, Sichuan.

brown. Maxillary palpus generally dark brown. Labial palpus generally pale yellow; basal segment tiny, second segment nearly as long as distal segment; distal segment fusiform, mostly dark brown, basally pale yellow. Mandibles yellowish-brown with distal half dark reddish-brown.

Thorax dark brown, yellowish-brown and pale yellow. Pronotum dark brown with pale yellowish markings, nearly broader than long, covered with many pale setae and a few dark setae; anteriorly with pair of pale yellowish spots; medially with longitudinal pale yellowish stripe; lateral margin pale yellow; pale yellow part of lateral margin wide. Mesoprescutum dark brown, with pair of brown markings; mesonotum dark brown, medially brown, mediolaterally with pair of longitudinal brown stripes, lateral margin with pair of brown spots; mesoscutellum dark brown, laterally with pair of pale yellowish spots, medially with longitudinal pale yellowish stripe, posterior margin pale yellow. Metanotum dark brown, with pair of reddish-brown markings; metascutellum dark brown, posteriorly with trident-shaped pale yellowish marking. Meso- and metapleura generally dark brown (Fig. 4C).

Legs yellow with dark brown markings, with some dark setae. All femora and tibiae ventrally with dark brown stripe; tibial spurs brown, spinous, shorter than tarsomere 1; tarsomeres generally yellow, dark brown distally; pretarsal claws slightly curved, barely protruded basally (Fig. 8C). Fore coxa yellow with some dark markings; middle and hind coxae generally dark brown.

Wings narrow, unmarked. Veins pale yellow, yellowish-brown and dark brown. Pterostigma pale. Sc generally with alternating pale yellow and dark brown in basal half, fully pale yellow in distal half; R fully yellowish-brown; marginal veins dark brown (Fig. 8A). Forewing CuA with alternating pale yellow and dark brown spots before forked; RP originating distad of MP and CuA fork; 9–11 presectoral crossveins present; RP with 9–10 branches; anterior Banksian line absent, posterior Banksian line present. Hindwing CuA generally pale yellow; five presectoral crossveins present; Banksian line absent (Figs 2B–C; 3A–B; 4A).

Abdomen dark brown with yellowish-brown markings. Terga 3–8 each medially with slender longitudinal yellowish-brown stripe (Figs 3A–B, 4A, 8E).

Male genitalia. Tergum 9 broad, nearly as long as wide in lateral view, anterior 2/3 dark brown, posterior 1/3 yellowish-brown. Sternum 9 dark brown, narrowly scallop-shaped, with long dark setae (Figs 3D–E). Anterior gonocoxites 9 slender, forming V-shaped structure in ventral view, wide in lateral view; posterior gonocoxites 9 small, coniform. Gonocoxites 11 slender round-arched; gonostyli 11 slightly protruding; gonapophyses 11 strongly sclerotized, subtriangular in lateral view (Figs 4H–L, 8G). Ectoproct modified, posteroventrally forming hook-like projection, with many long setae (Figs 4D–E).

Female genitalia. Pregenital plate tiny, coniform. Anterior branches of gonocoxites 8 tubercular, with some stout spiculate short setae; posterior branches of gonocoxites 8 slender digitiform, distally with some stout setae. Gonocoxites 9 basally with dense short stout setae, distally with some stout and blunt setae. Ectoproct rounded on distal margin, posteroventrally with some stout and blunt setae (Figs 4F–G).

3rd instar larva. *Size*. Body length (excluding mandible): 5.37–7.96 mm; head length: 1.68–2.94 mm; head width 1.21–2.02 mm; mandible length: 1.73–3.12 mm.

Head nearly trapezoidal in dorsal view, longer than wide, basally narrower. Clypeo-labrum generally dark brown in dorsal view, with row of setae. Head pale yellow; in dorsal view, anteromedially with pair of close black spots, medially with pair of lung-form dark brown markings, laterally with pair of dark brown markings; in ventral view, anteromedially with pair of large subtriangular dark brown markings, mediolaterally with pair of dark brown spots. Mandible as long as head, mostly pale yellow, distally reddish-brown, equipped with three pairs of teeth, basally pale yellow, distally reddish-brown and gradually darkened on tip. Second tooth nearly longer than first tooth, third tooth nearly longer than second tooth. Six to seven interdental mandibular setae present anterior to first tooth; two to three interdental mandibular setae between first and second tooth; two interdental mandibular setae between second and third tooth; one to two interdental mandibular setae distad of third tooth. External margin of mandible with three groups of long, relatively short, and tiny setae, respectively (Figs 5A–C, 9A–B).

Thorax. Pronotum pale yellow, with pair of longitudinal wide dark brown stripes; lateral margin with many long setae and dorsally with some tiny setae; ventral prothorax with pair of dark brown markings. Mesothorax dorsally with spiracles present on reduced brown sclerotized tubercle; meso- and metathorax dorsally with many dark brown spots and dots; meso- and metathoracic setiferous processes reduced, with dense long setae; mesothorax ventrally with pair of dark brown markings and metathorax ventrally with two pairs of dark brown markings (Figs 5A–C, 9E).

Legs pale yellow. All legs coxa basally with dark brown marking, covered with some long and short setae; femur and tibia with a few long setae and many short setae. Middle femur 1.5× as long as fore femur (Figs 5A–C).

Abdomen pale yellow, with many dark brown markings. Dorsal segments 1–8 each medially with longitudinal dark brown marking and laterally with two pairs of abreast dark brown markings, suffused with many dark brown dots (Fig. 5A). Ventral segments 1–8 each medially with dark brown dot and pair of dark brown markings (Fig. 5B). Segment 8 odontoid processes pale brown, tiny. Segment 9 nearly half as long as wide, posteriorly with four digging setae forming transversal row; sometimes one or two sclerotized setae present anterior to the transversal row of digging setae; rastra reduced, each rastrum equipped with four digging setae of which external one nearly twice as long as internal setae (Fig. 9G).

Etymology. This new species is named after the mountain range it inhabits, i.e., the Shaluli mountain range; adjective.

Bio-ecology. Like other *Myrmeleon* larvae, the larvae of this new species make pit-shaped traps to ambush prey (Fig. 1C) but they are restricted to the mid-elevation

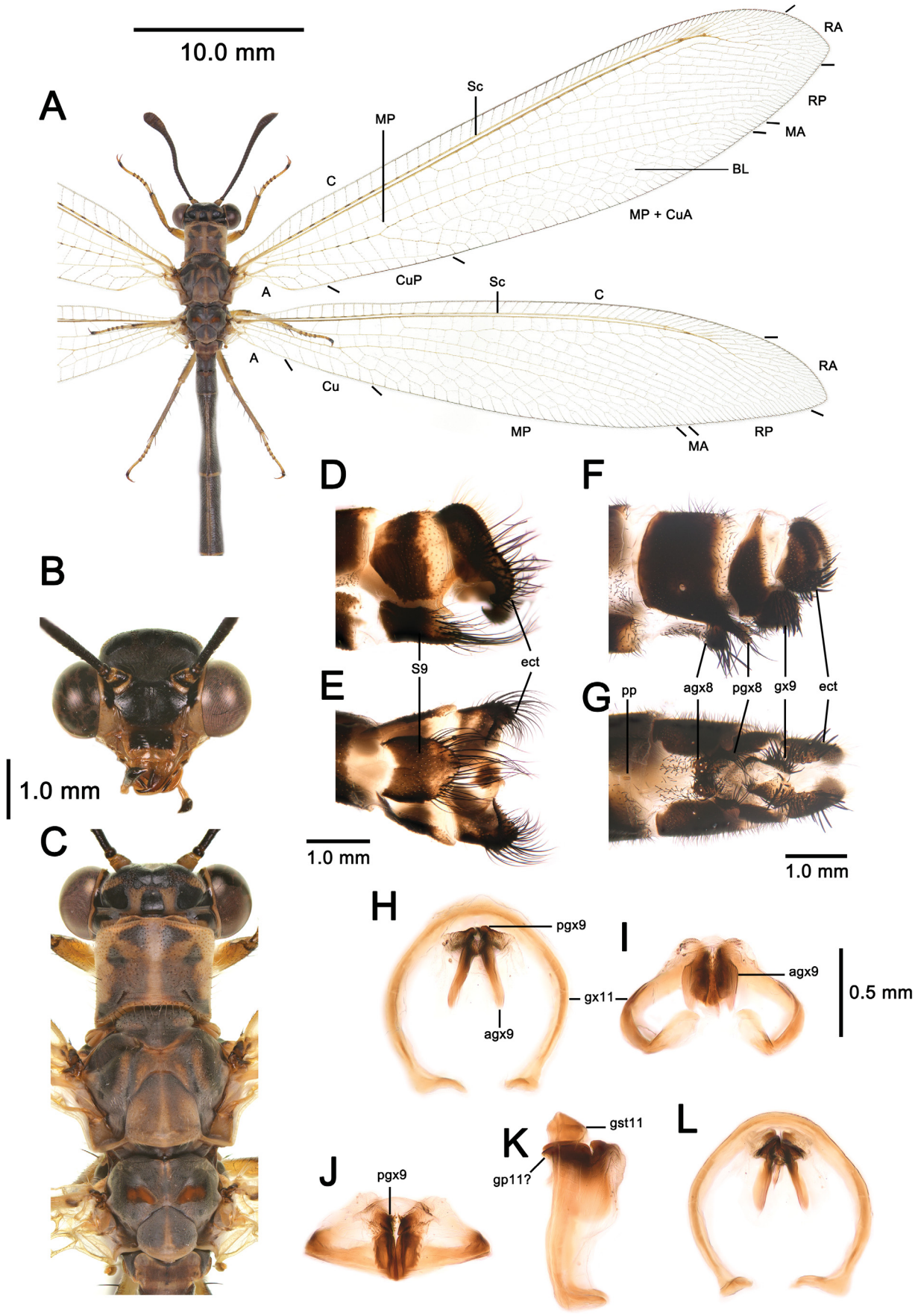

Fig. 4. *Myrmeleon shalulianus* Zheng & Liu sp. nov., adult. A – part of habitus; B – head, frontal view; C – head and thorax, dorsal view; D–E – male terminalia (D – lateral view, E – ventral view); F–G – female terminalia (F – lateral view; G – ventral view); H–L – male genitalia (H – ventral view, I – anteroventral view, J – caudal view, K – lateral view, L – dorsal view).

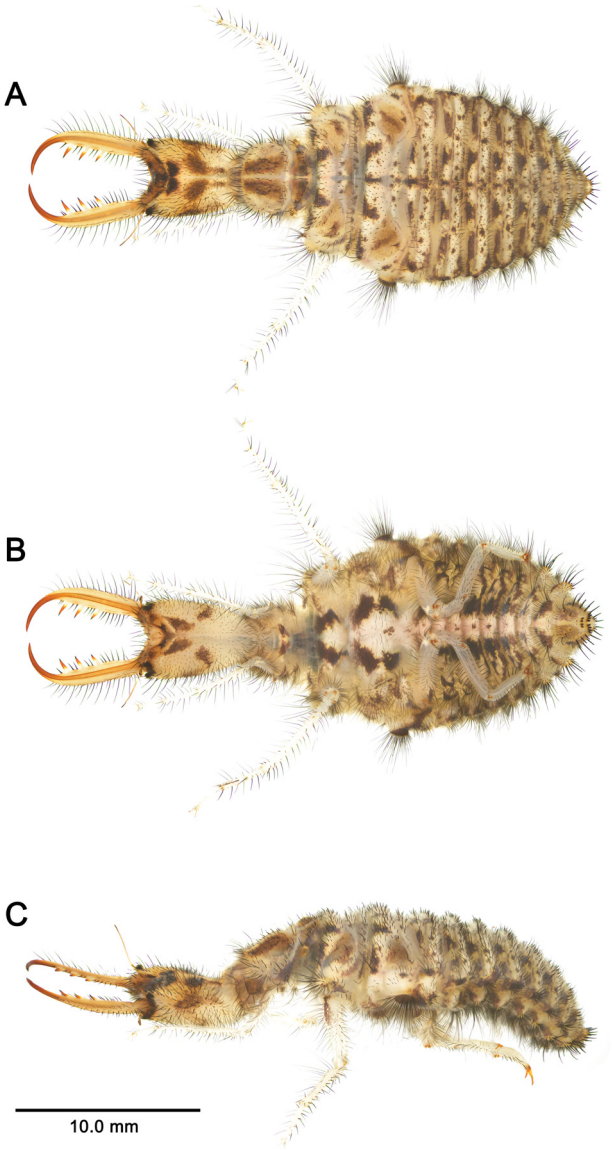

Fig. 5. *Myrmeleon shalulianus* Zheng & Liu sp. nov., habitus of 3rd instar larva: A – dorsal view, B – ventral view, C – lateral view.

dry-hot river valleys of the Jinshajiang River from the Shaluli mountain range (Figs 1E, G).

Distribution. China (Sichuan, Yunnan).

Comparative notes. This new species is closely related to *M. trigonois*, so when *M. trigonois* was previously published, the specimens of this new species were treated as paratypes of *M. trigonois*. However, there are significant differences between them. In *M. shalulianus* sp. nov., the dark brown marking on gena is only present on the anterior part (Fig. 4B); the pale yellowish part of the lateral margin of pronotum is wider than in *M. trigonois* (Fig. 4C); the mesoscutellum has a pair of pale yellow spots laterally (Fig. 4C); the hind femur is yellow dorsally; the tarsomeres are generally yellow, only distal parts are dark brown (Fig. 8C); the wing veins are generally pale yellow and yellowish-brown; Sc is generally with alternating pale yellow and dark brown in basal half, and is fully pale yellow in distal half; R is fully yellowish-brown (Figs 2B–C, 3A–B, 4A, 8A); stripes on each abdominal terga 3–8 are narrower (Figs 3A–B, 4A, 8E); male anterior gonocoxites 9 are slender and forming a V-shaped structure in ventral view; male posterior gonocoxites 9 are small, coniform; male gonocoxites 11 are slender round-arched (Figs 4H–L, 8G); the anteromedial pair of markings on the ventral side of larval head is larger (Fig. 9B).

However, in *M. trigonois*, an internal black stripe on gena extends to the posterior part (Fig. 6B); the pale yellowish part of the lateral margin of pronotum is narrower than in *M. shalulianus* sp. nov. (Fig. 6C); the mesoscutellum only has a longitudinal pale yellow stripe medially, the lateral pair of spots is absent; the hind femur is mostly dark brown dorsally (Fig. 6C); tarsomere 5 is generally dark brown; the wing veins are generally pale and dark brown (Fig. 8D); Sc is generally with alternating pale and dark brown; R is generally with alternating pale brown and dark brown (Figs 2A, 3C–D, 6A, 8B); stripes on each abdominal terga 3–8 are broader (Figs 3C–D, 6A, 8F); male anterior gonocoxites 9 are short coniform; male posterior gonocoxites 9 are nearly long trapezoid in ventral view; male gonocoxites 11 are wide round-arched (Figs 6H–L, 8H); the anteromedial pair of markings on the ventral side of larval head is smaller (Fig. 9D). Besides, our DNA barcoding evidence also confirms that *M. shalulianus* sp. nov. and *M. trigonois* are two different species (see Molecular identification; Fig. 13; Table 2).

Remark. Based on our examination of the type specimens of *M. trigonois* (Fig. 2), we treat all paratypes of *M. trigonois* as the paratypes of *M. shalulianus* sp. nov.

Myrmeleon trigonois Bao & Wang, 2006

Chinese common name: 角蚁蛉

(Figs 1B, D; 2A, C; 3C–D; 6; 7; 8B, D, F, H; 9C–D, F, H; 13; 14)

Myrmeleon trigonois Bao & Wang, 2006: 129 (type locality: China: Yunnan, Diqing, Deqen County, Meilishi Village; holotype in CAU). Yang et al. (2018): 67 (*Myrmeleon*); Wang et al. (2018): 102 (*Myrmeleon*).

Type material examined. Holotype: ♂, **CHINA: Yunnan:** Diqing, Deqen County [德钦县], Meilishi [梅里石], 2200 m, 20.VII.1982, Shuyong Wang (CAU).

Additional material examined. CHINA: Chongqing: 1 ♀, Beibei District [北碚区], Mt. Jinyunshan [缙云山], 8–14.vii.2020, Qiaoqiao Liu (CAU); 1 ♀ (reared to adult, emerged in 17.x.2021), same locality as above, 1.viii.2021 (CAU); 1 ♀, Wushan County [巫山县], Dangyang Township [当阳乡], Wulipo National Natural Reserve [五里坡国家级自然保护区], 1753 m, 21.vii.2021, Lulan Jie (CAU); 1 ♀ (reared to adult, emerged in 19.vii.2023) and 2 3rd instar larvae, Wuxi County [巫溪县], Lanying Township [兰英乡], Lanying Village [兰英村], 900 m, 17.v.2023, Yuchen Zheng (CAU). **Shaanxi:** 1 ♀, Hanzhong, Liuba County [留坝县], 23.vi.2012, Hui Wen (CAU). **Sichuan:** 6 ♀♀ (reared to adult, emerged in 20.vi–2.ix.2023) and 7 3rd instar larvae, Aba, Wenchuan County [汶川县], Weizhou Town [威州镇], Qiangrengu [羌人谷], 1500–1700 m, 11–12.v.2023, Yuchen Zheng (CAU); 1 ♀ (reared to adult, emerged in 28.vii.2023), Aba, Lixian County [理县], Taoping Town [桃坪镇], 12.v.2023, Yuchen Zheng (CAU); 1 ♂ (reared to adult, emerged in 27.v.2021) and 4 larvae, Garze, Danba County [丹巴县], Zhake Village [扎科村], Ripo [日坡], 1500 m, 12.iv.2021, Yuchen Zheng (CAU); 1 ♀ and 4 2nd instar larvae, Guangyuan, Lizhou District [利州区], Zoumaling [走马岭], Longhao Aviation School [龙昊职业航校], 550 m, 23.viii.2023, Wenkai Kou (CAU); 1 ♂, Panzhihua, West District, National Nature Reserve of Cycad *Cycas panzhihuaensis* [攀枝花苏铁国家级自然保护区], 1508 m, 12.vii.2015, Lu Yue (CAU). **Yunnan:** 1 ♀ (reared to adult), Dali, Mt. Cangshan Geopark of Dali [大理苍山

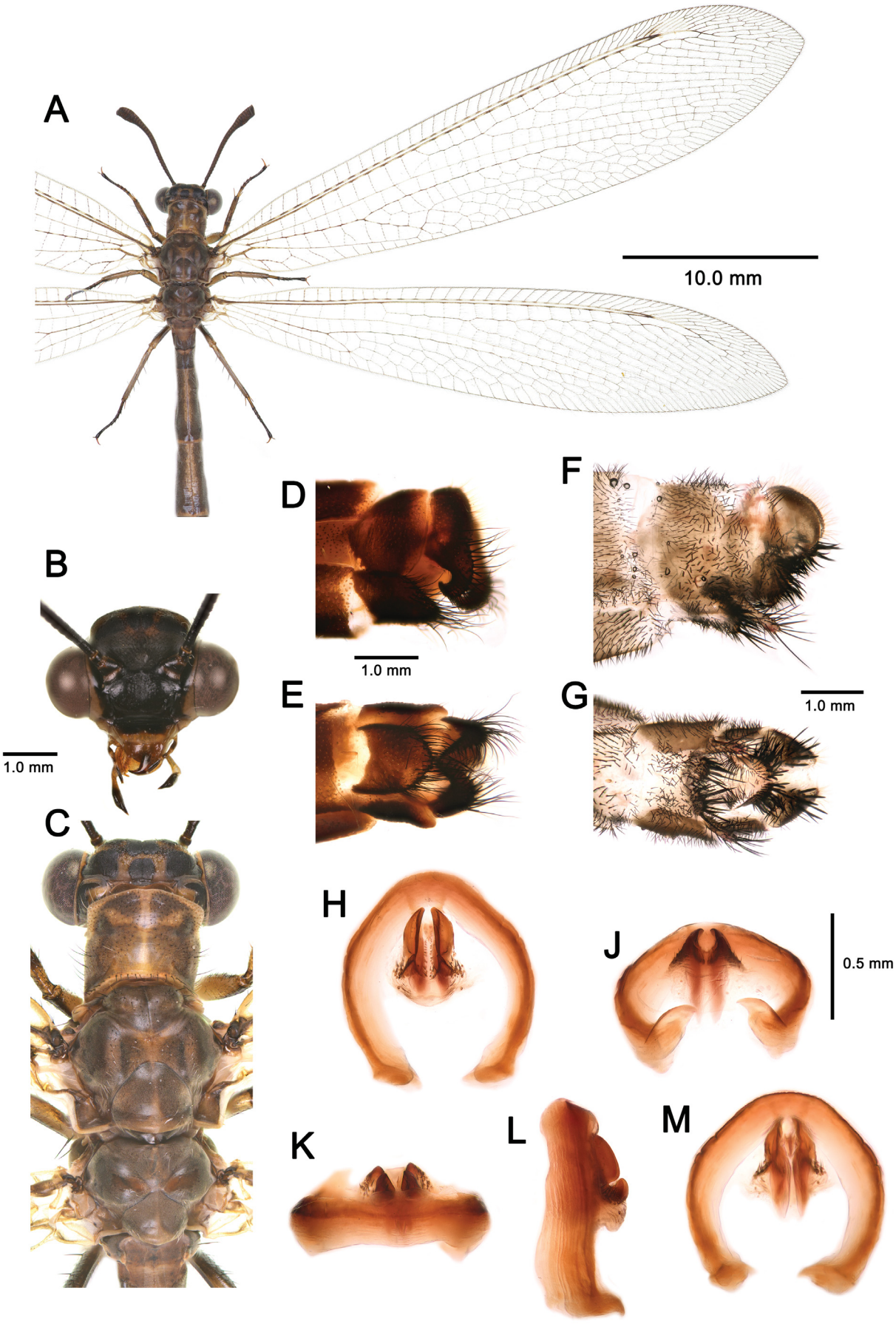

Fig. 6. *Myrmeleon trigonois* Bao & Wang, 2006, adult. A – part of habitus; B – head, frontal view; C – head and thorax, dorsal view; D–E – male terminalia (D – lateral view, E – ventral view); F–G – female terminalia (F – lateral view; G – ventral view); H–L – male genitalia (H – ventral view, I – anteroventral view, J – caudal view, K – lateral view, L – dorsal view).

地质公园], 2200 m, Jialing Li & Jishen Wang (CAU); 1 ♂, Zhaotong, Suijiang County [绥江县], Mt. Fengdingshan [峰顶山], 16.ix.2009, Cao, Yang & Liu (CAU).

Diagnosis. ***Adult.*** Gena mostly pale yellow, with an internal black stripe extending to posterior part (Fig. 6B). Pale yellowish part of the lateral margin of pronotum narrow. Mesoscutellum only with a longitudinal, pale yellow stripe (Fig. 6C). Hind femur generally dark brown dorsally. Tarsomere 5 generally dark brown (Figs 6A, 8D). Wing veins generally pale and dark brown; Sc generally with alternating pale and dark brown; R generally with alternating pale brown and dark brown (Figs 2A, C; 3C–D; 6A; 8B). Abdominal terga 3–8 each medially with a wide longitudinal yellowish-brown stripe (Figs 3C–D, 6A, 8F). Male anterior gonocoxites 9 short coniform, posterior gonocoxites 9 nearly long trapezoid in ventral view; gonocoxites 11 wide round-arched (Figs 6H–L, 8H).

Larva. Head anteromedially with a pair of small subtriangular dark brown markings in ventral view (Figs 7B, 9D).

Description. ***Adult.*** *Size*. Head width: 2.51–2.72 mm; forewing length: 31.12–34.94 mm; hindwing length: 31.74–35.73 mm.

Head. Vertex raised, black, anteriorly with brown annular marking, laterally with pair of brown markings. Antennae generally black (Fig. 6C). Gena wide, pale yellow, with internal black stripe extending to posterior part (Fig. 6B). Frons mostly black. Clypeus anterior 2/3 black, posterior 1/3 pale yellow (Fig. 6B). Labrum brown. Maxillary palpus generally dark brown. Labial palpus generally pale yellow; basal segment tiny, second segment nearly as long as distal segment; distal segment fusiform, mostly dark brown, basally pale yellow. Mandibles yellowish-brown with distal half dark reddish-brown.

Thorax dark brown, yellowish-brown and pale yellow. Pronotum dark brown with pale yellowish markings, nearly broader than long, covered with many pale setae and a few dark setae; anteriorly with pair of pale yellowish spots; medially with longitudinal pale yellowish stripe; lateral margin pale yellow; pale yellow part of lateral margin narrow. Mesoprescutum dark brown, sometimes with pair of brown markings; mesonotum dark brown, medially brown, mediolaterally with pair of longitudinal brown stripes, lateral margin with pair of brown spots; mesoscutellum dark brown, medially with longitudinal pale yellowish stripe. Metanotum dark brown, with pair of reddish-brown markings; metascutellum dark brown, posterior with trident-shaped pale yellowish marking. Meso- and metapleura generally dark brown (Fig. 6C).

Legs yellow with dark brown markings, with some dark setae. All coxae generally dark brown; tibiae ventrally with dark brown stripe; tibial spurs brown, spinous, shorter than tarsomere 1; pretarsal claws slightly curved, barely protruding basally (Fig. 6A). Fore leg: femur yellow, ventrally with longitudinal dark brown stripe; tarsomeres 1–4 generally yellow, dark brown distally, tarsomere 5 dark brown. Middle leg: femur yellow, ventrally with longitudinal dark brown stripe; tarsomere 1 generally brown, dark brown distally, tarsomeres 2–4 basally brown, distally dark brown, tarsomere 5 generally dark brown. Hind leg: femur generally dark brown, basally yellow and distally brown; tarsomere 1 generally brown, dark brown distally, tarsomeres 2–4 basally brown, distally dark brown, tarsomere (Fig. 8D).

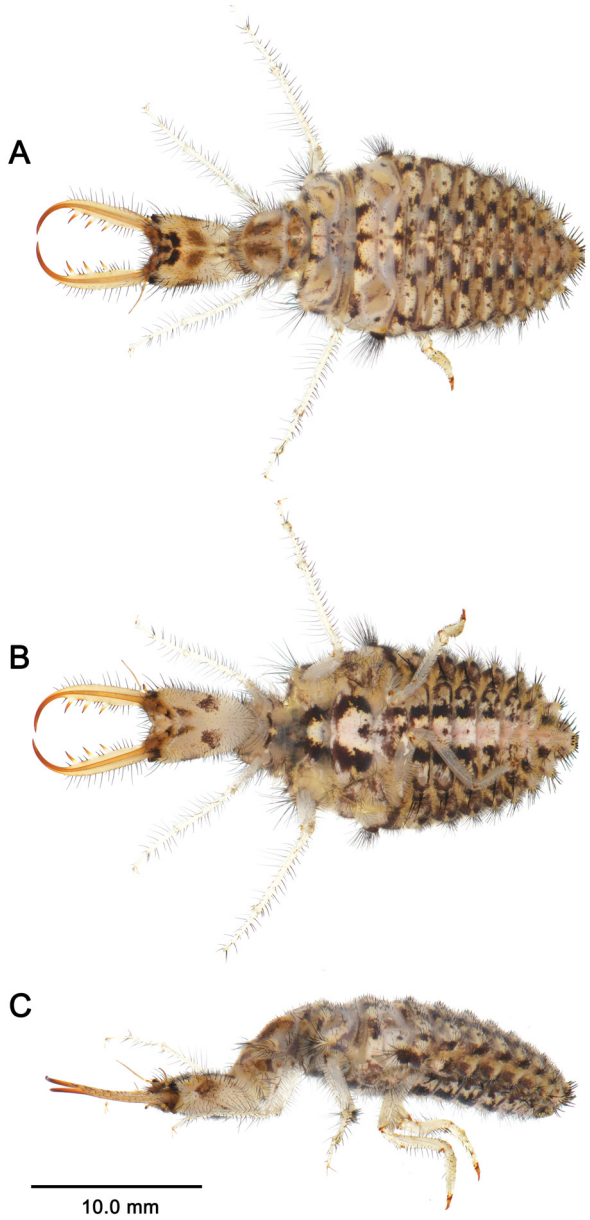

Fig. 7. *Myrmeleon trigonois* Bao & Wang, 2006, habitus of 3rd instar larva (A – dorsal view, B – ventral view, C – lateral view).

Wings narrow, unmarked. Veins pale and dark brown. Pterostigma pale, indistinct brown spot proximad of pterostigma. Sc generally with alternating pale and dark brown; R generally with alternating pale brown and dark brown; CuA with alternating pale yellow and dark brown; RP originating distad of MP and CuA fork (Fig. 8B). Forewing with 10–13 presectoral crossveins; RP with 9–10 branches; anterior Banksian line absent, posterior Banksian line present. Hindwing with six to seven presectoral crossveins; Banksian line absent (Figs 2A, C; 3C–D; 6A).

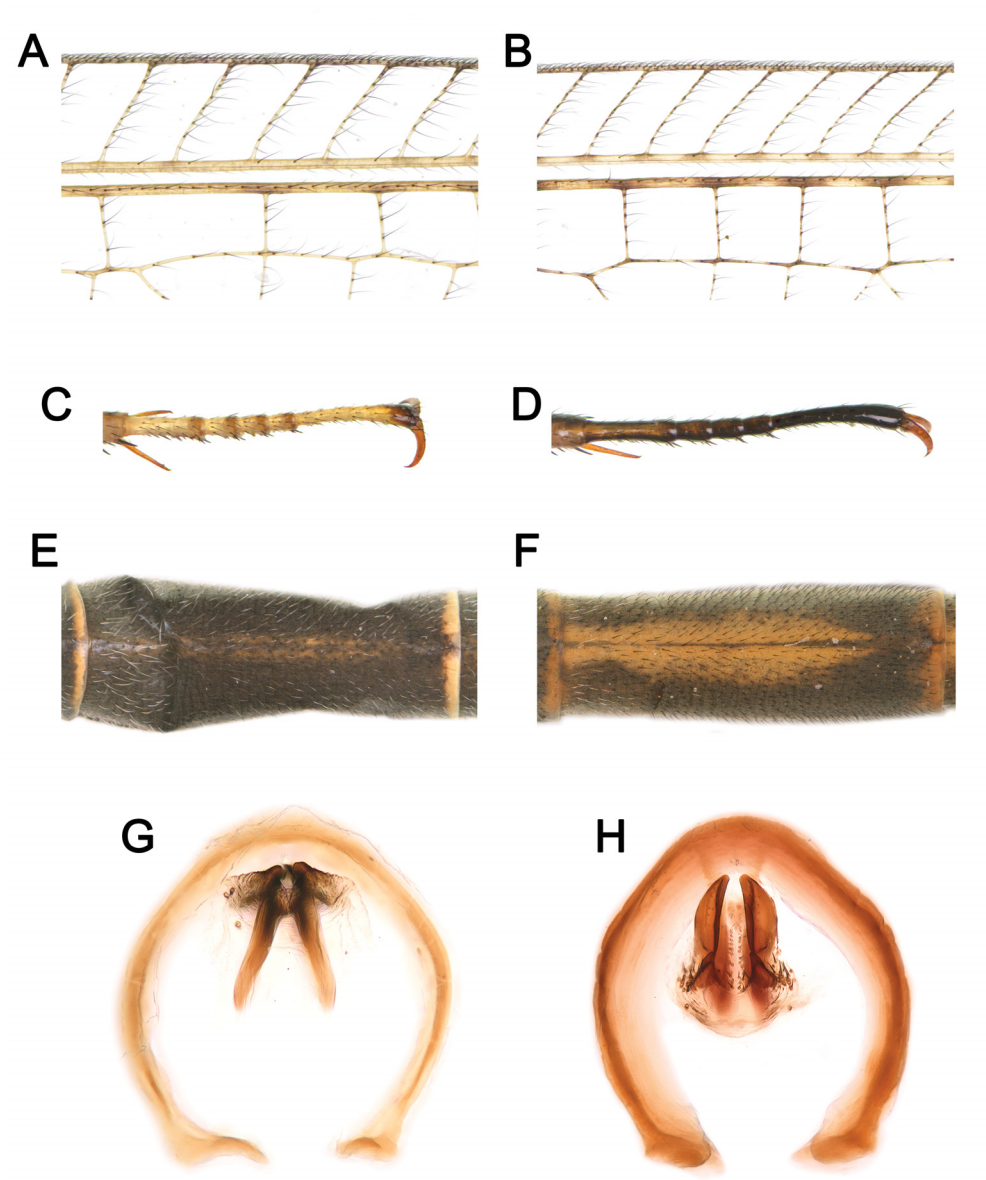

Fig. 8. Detailed comparison between *Myrmeleon shalulianus* Zheng & Liu sp. nov. (A, C, E, G) and *M. trigonois* Bao & Wang, 2006 (B, D, F, H). A–B – part of forewing; C–D – hind tarsus; E–F – abdominal tergum 4; G–H – male genitalia, ventral view.

Abdomen dark brown with yellowish-brown markings. Terga 3–8 each medially with wider longitudinal yellowish-brown stripe (Figs 3C–D, 6A, 8F).

Male genitalia. Tergum 9 broad, nearly as long as wide in lateral view, generally dark brown, posterior margin yellowish-brown. Sternum 9 dark brown, narrowly scallop-shaped, with long dark setae (Figs 6D–E). Anterior gonocoxites 9 short coniform; posterior gonocoxites 9 nearly long trapezoid in ventral view. Gonocoxites 11 wide round-arched; gonostyli 11 slightly protruded; gonapophyses 11 shaped as a pair of fusiform structures (Figs 6H–L, 8H). Ectoproct modified, posteroventrally forming a hook-like projection, with many long setae (Figs 6D–E).

Female genitalia. Pregenital plate tiny, and coniform. Anterior branches of gonocoxites 8 tubercular, with some stout spiculate setae; posterior branches of gonocoxites 8 slender digitiform, distally with some stout setae. Gonocoxites 9 basally with dense short stout setae, distally with some stout and blunt setae. Ectoproct rounded on distal margin, posteroventrally with some stout and blunt setae (Figs 6F–G).

3rd instar larva. *Size*. Body length (excluding mandible): 6.17–8.78 mm; head length: 1.76–3.66 mm; head width 1.38–2.69 mm; mandible length: 1.92–3.96 mm.

Head nearly trapezoidal in dorsal view, longer than wide, basally narrower. Clypeo-labrum generally dark brown in dorsal view, with row of setae. Head pale yellow; in dorsal view, anteromedially with pair of close black spots, medially with pair of lung-form dark brown markings, laterally with pair of dark brown markings; in ventral view, anteromedially with pair of small subtriangular dark brown markings, mediolaterally with pair of dark brown spots. Mandible as long as head, mostly pale yellow, distally reddish-brown, equipped with three pairs of teeth, basally pale yellow, distally reddish-brown and gradually darkened on tip. Second tooth nearly longer than first tooth,

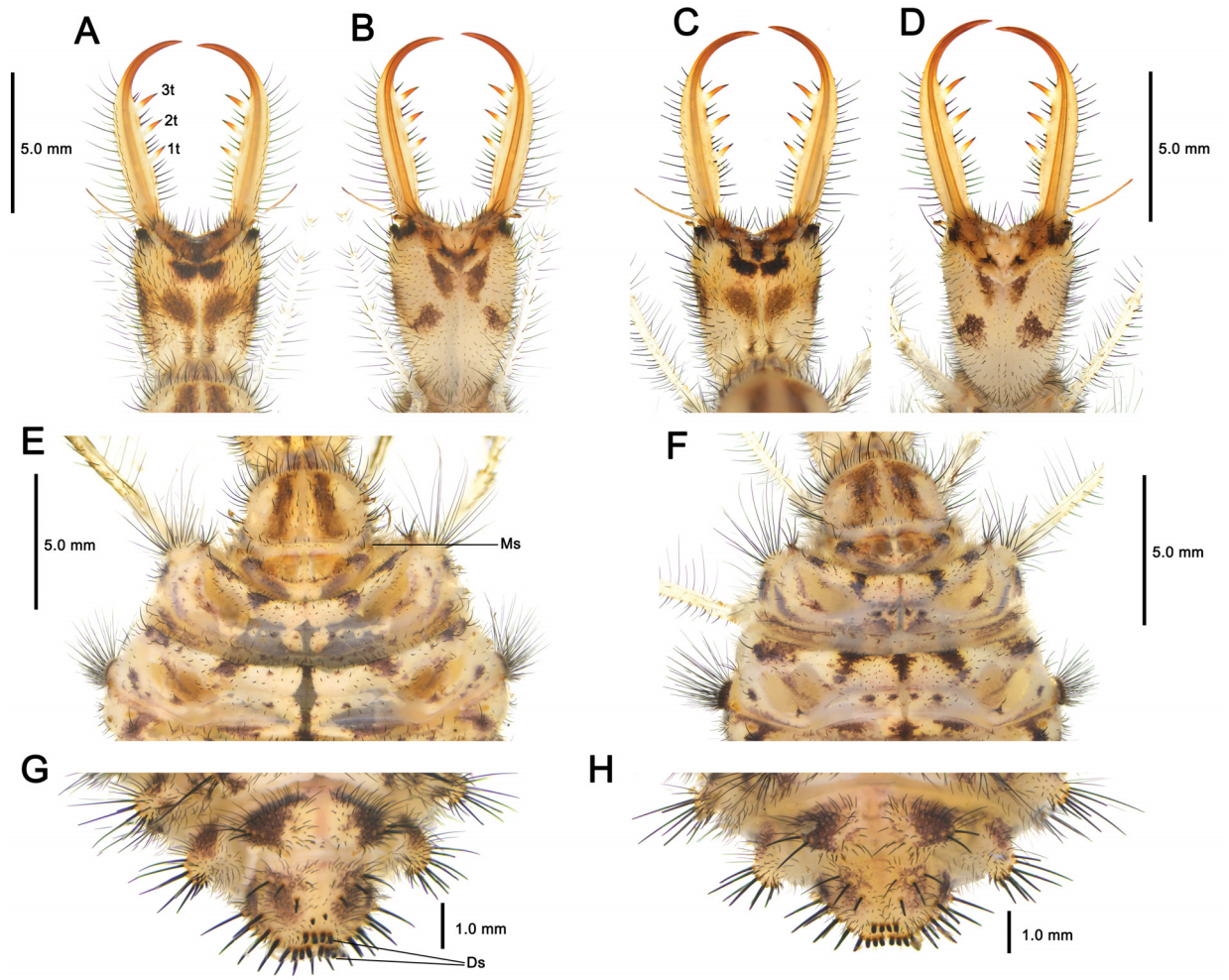

Fig. 9. 3rd instar larvae of *Myrmeleon shalulianus* Zheng & Liu sp. nov. (A–B, E, G) and *M. trigonois* Bao & Wang, 2006 (C–D, F, H): A, C – head, dorsal view; B, D – head, ventral view; E–F – thorax, dorsal view; G–H – abdominal segments 8–9, ventral view.

third tooth nearly longer than second tooth. Five to seven interdental mandibular setae present anterior to first tooth; two to three interdental mandibular setae between first and second tooth; two interdental mandibular setae between second and third tooth; one to two interdental mandibular setae distad of third tooth. External margin of mandible with three groups of long, relatively short, and tiny setae respectively (Figs 7A–C, 9C–D).

Thorax. Pronotum pale yellow, with pair of longitudinal wide dark brown stripes; lateral margin with many long setae and dorsally with some tiny setae; ventral prothorax with pair of dark brown markings. Mesothorax dorsally with spiracles present on reduced brown sclerotized tubercle; meso- and metathorax dorsally with many dark brown spots and dots; meso- and metathoracic setiferous processes reduced, with dense long setae; mesothorax ventrally with pair of dark brown markings and metathorax ventrally with two pairs of dark brown markings (Figs 7A–C, 9F).

Legs pale yellow. All legs with coxa unmarked, covered with some long and short setae; femur and tibia with a few long setae and many short setae. Middle femur 1.5× as long as fore femur (Figs 7A–C).

Abdomen pale yellow, with many dark brown markings. Dorsal segments 1–8 each medially with longitudinal dark brown marking and laterally with two pairs of not abreast dark brown markings, suffused with many dark brown dots (Fig. 7A). Ventral segments 1–8 each medially with dark brown dot and pair of dark brown markings (Fig. 7B). Segment 8 odontoid processes pale brown, tiny. Segment 9 nearly half as long as wide, posteriorly with four digging setae forming transversal row; sometimes one or two sclerotized setae present anterior to the transversal row of digging setae; rastra reduced, each rastrum equipped with four digging setae of which external one nearly twice as long as internal setae (Fig. 9H).

Bio-ecology. Like other *Myrmeleon* larvae, the larvae of this new species make pit-shaped traps to ambush prey (Fig. 1D). This species is widespread in moist, low- to mid-elevation, densely vegetated mountains from the Yunling mountain range to the Wushan mountain range (Figs 1F, H).

Distribution. China: Chongqing (this paper), Shaanxi (this paper), Sichuan (this paper), Yunnan (Bao & Wang 2006, this paper).

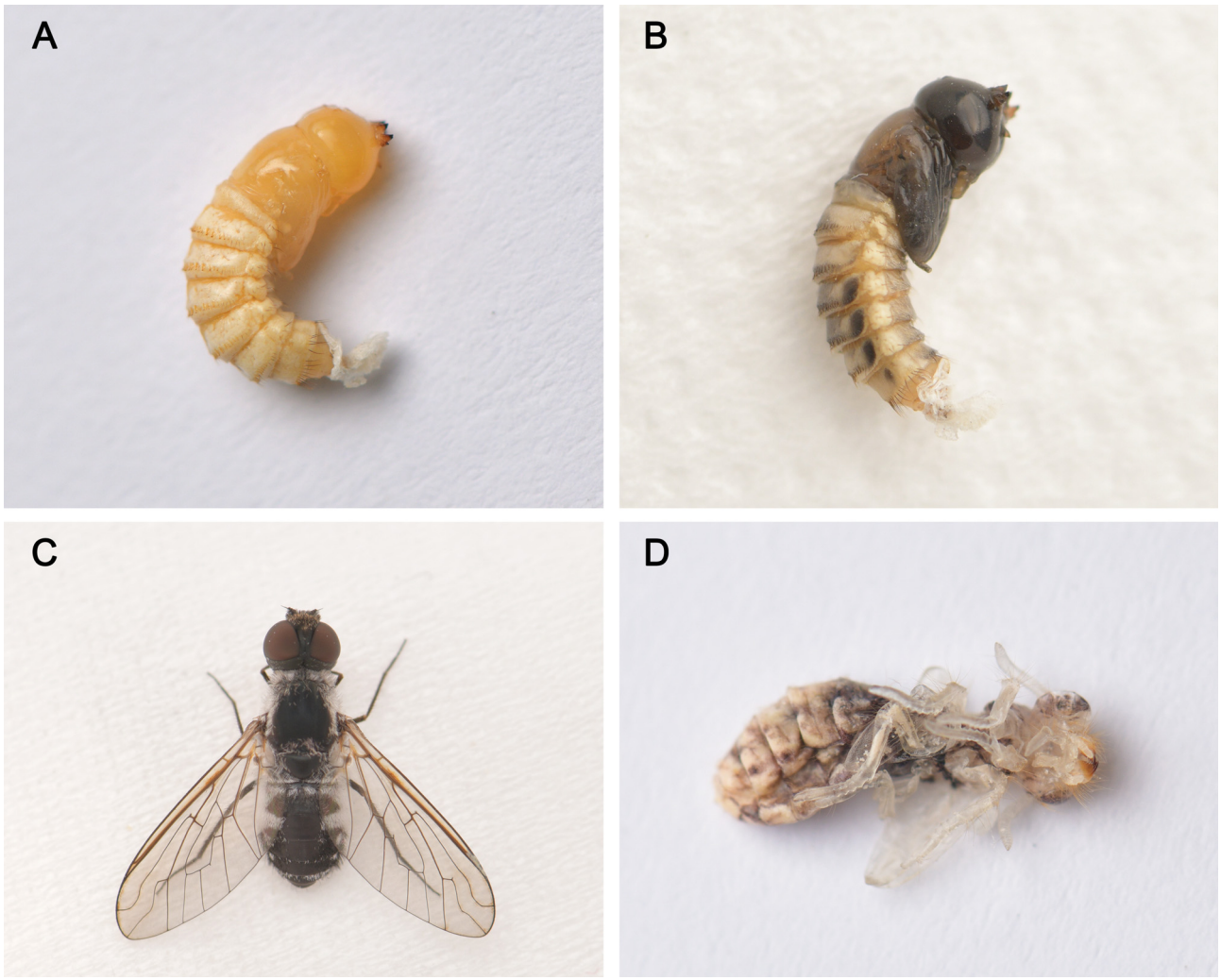

Fig. 10. Parasitoid *Taiwanon* sp. (Diptera: Bombyliidae) and parasitism of *Myrmeleon trigonois* Bao & Wang, 2006. A – pupa of *Taiwanon* sp., lateral view; B – pupa of *Taiwanon* sp., ready to emerge; C – living adult of *Taiwanon* sp.; D – remains of *M. trigonois* pupa (photos by Yuchen Zheng).

Order Diptera Linnaeus, 1758

Family Bombyliidae Latreille, 1802

***Taiwanon* sp.**

Chinese common name: 台蜂虻

(Figs 10–12)

Material examined. CHINA: Chongqing: 2 ♀♀ (emerged 3.viii.2023 from larvae of *Myrmeleon trigonois*), Wuxi County, Lanying Township, Lanying Village, 900 m, 17.v.2023, Yuchen Zheng (CAU).

Description. ***Adult (female).*** *Head* about 1.5× wider than long, mostly black with sparse pale pruinescence and covered in short black hairs and short white to pale yellow scales. Eyes dichoptic. Frons triangular with sparse pale pruinescence, 9.0× length of ocellar tubercle, 3.1× as wide as ocellar tubercle, upper half with short black hairs; lower half as long as upper half, with admixed short black hairs and short pale yellow scales. Ocellar tubercle slightly raised, blackish brown to black with sparse grey pruinescence, with short blackish hairs. Face with thick pale pruinescence and admixed short black hairs and short white to pale yellow scales, denser than frons but dorsal lateral area (below antenna) bare. Gena narrow, with thick pale pruinescence. Clypeus with thick pale pruinescence and otherwise bare. Occiput with thick pale pruinescence and sparse short white scales, margin of cavity with admixed dense short white scales and sparse short black hairs. Posterior eye margin deeply indented with narrow line dividing facets. Antenna black with thick brownish pruinescence, scape and pedicel with short black hairs, hairs denser and longer ventrally; flagellum bare. Scape 1.9× as long as wide, and 2.8× as long as pedicel, uniform from base to apex. Pedicel 0.8× as long as wide. Flagellum 12.0× as long as wide, 1.2× as long as scape + pedicel, 1.3× as long as scape, one-segmented with apical stylus. Palpus rudimentary, not extending beyond oral cavity, yellow with apically black, with short black hairs, one-segmented, without palpal pit. Mouthparts slender, not extending beyond oral cavity, brownish yellow with short brownish hairs.

Thorax. Integumental colour of scutum mostly black with sparse grey pruinescence. Scutum covered with white scales, hairs denser marginally, without distinct bristles. Scutellum black with sparse grey pruinescence, covered with short white scales. Pleura black with thick grey pruinescence, proepisternum densely covered in long black hairs, posterodorsal half of anepisternum with admixed dense long white scales and sparse black hairs, anteroventral area of anepisternum with black hairs, ka-

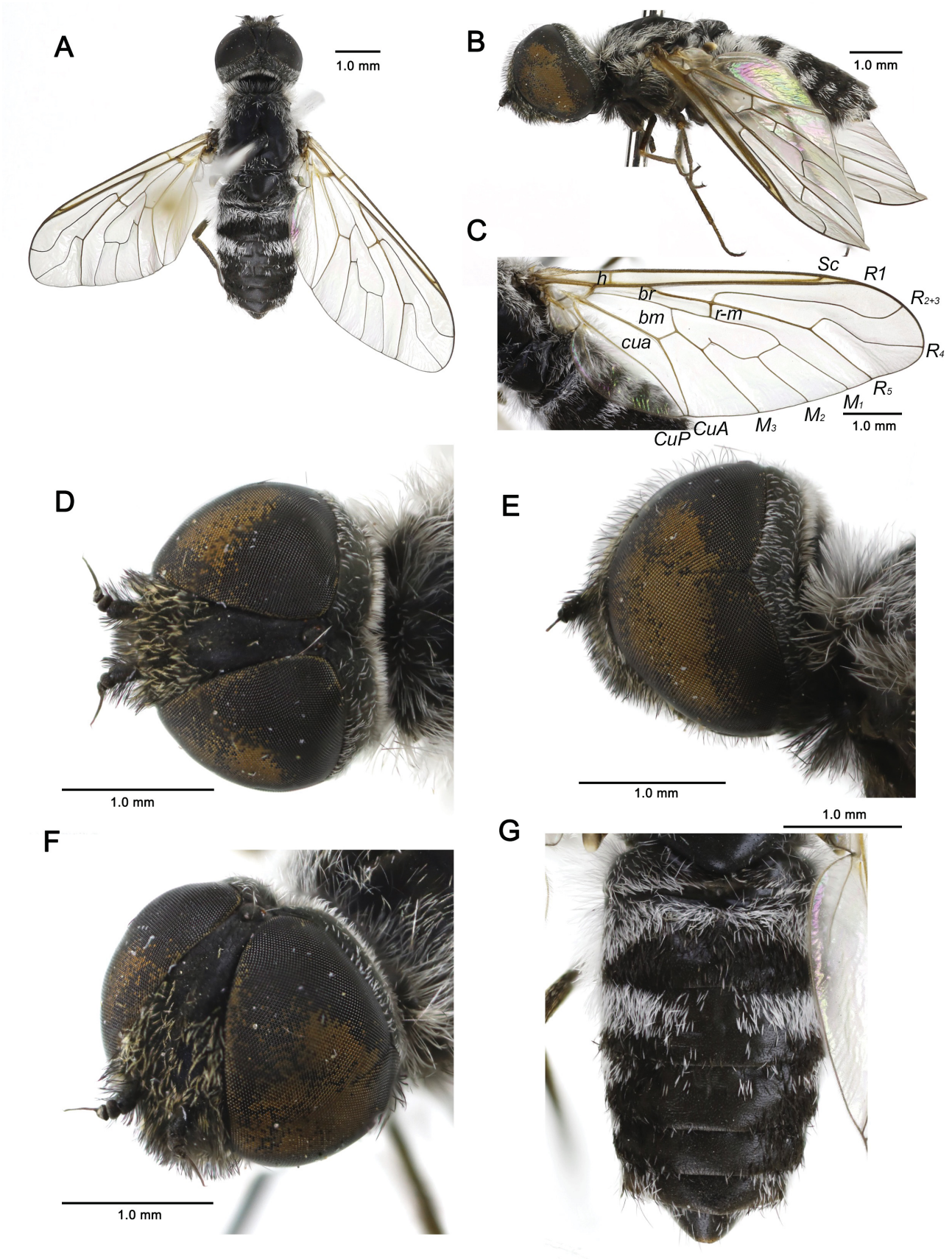

Fig. 11. *Taiwanon* sp., female. A – dorsal view; B – lateral view; C – wing; D – head, dorsal view; E – head, lateral view; F – head, lateral view; G – abdomen, dorsal view. (Photos by Haoyue Zhou).

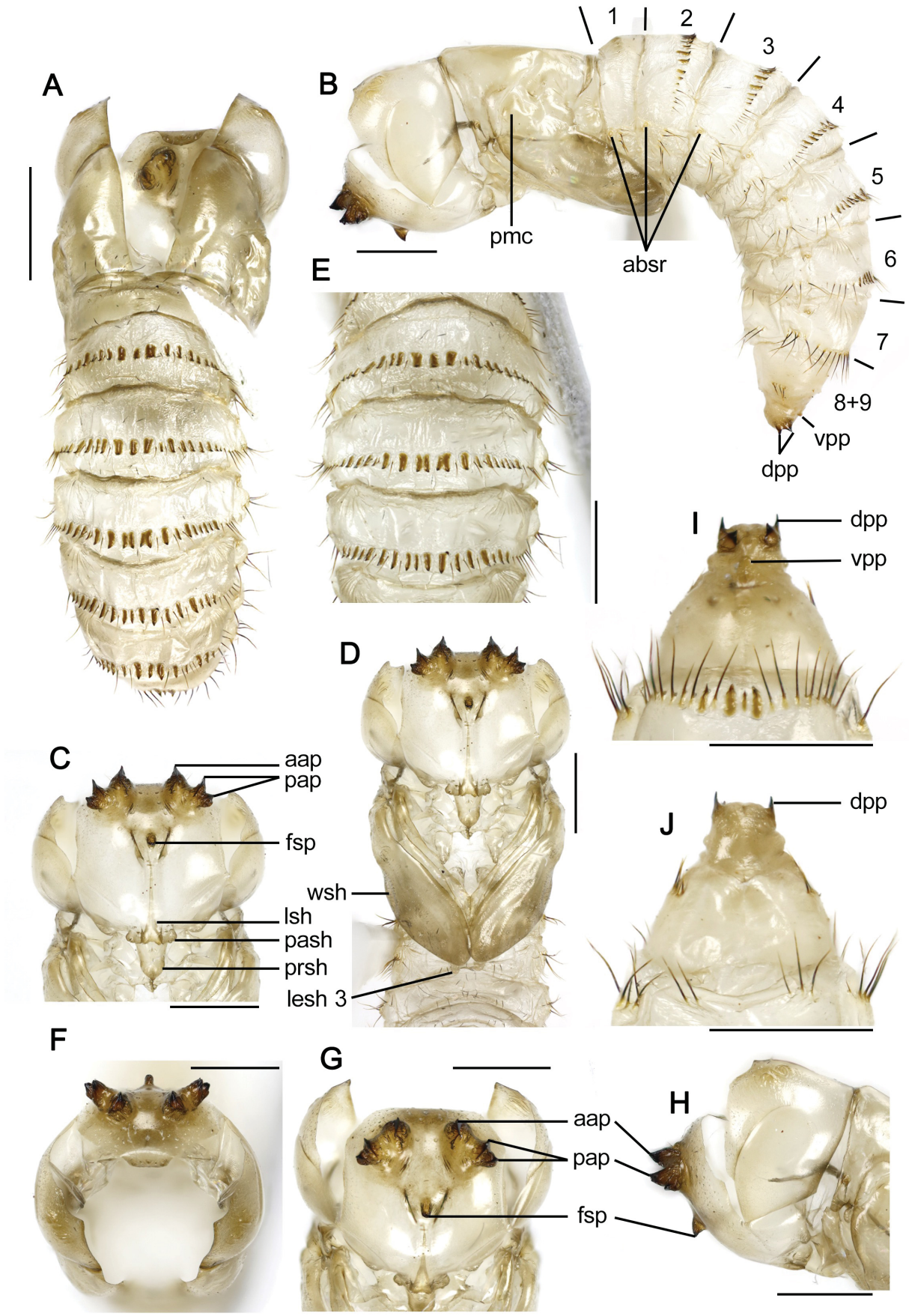

Fig. 12. *Taiwanon* sp., female pupal exuvia. A – dorsal view; B – lateral view; C – head, ventral view; D – head and thorax, ventral view; E – abdominal segments 2–4, dorsal view; F – cephalic spines, dorsal view; G – cephalic spines, frontal view; H – cephalic spines, lateral; I – anal segment, dorsal view; J – anal segment, ventral. (Photos by Haoyue Zhou).

tepisternum with black hairs and ventral half admixed with pale yellow scales, anepimeron with pale yellow scales and black hairs, laterotergite and mediotergite with dense long white scales, proepimeron, meron, and metapleuron bare.

Legs mostly brown except for blackish brown femora, femora mostly covered in yellow scales and ventral half with black hairs, tibia mostly covered in blackish brown scales, except for ventroposterior face of middle femur that is covered with dense long white and black hairs. Bristles on legs black. Fore tibia 3.5× longer than fore basitarsus, middle tibia 3.1× longer than middle basitarsus, hind tibia 3.0× longer than hind basitarsus.

Wings. Wing membrane hyaline. Cell r5 open; cell br longer than cell bm, R2+3 arising from R4+5 right before crossvein r-m, crossvein r-m arising from basal half of cell dm; cell cua open (Fig. 11D). Stump vein present on R2+3, R4, and crossvein m-m (Fig. 11D). Haltere stem and knob blackish brown.

Abdomen. Integumental color of tergites black mostly with sparse grey pruinescence. Tergite 1 with dense white hairs and scales; tergites 2–3 with white scales and hairs on anterior half and black scales and hairs on posterior half; tergites 4–7 with black scales and laterally admixed with white scales. Sternites black with thick pale pruinescence, covered in black hairs and scales, laterally admixed with white scales.

Male. Unknown.

Pupal exuviae. Length: 9.0–11.0 mm. Head width: 1.7–2.0 mm. Thorax width: 2.3–2.8 mm. Abdominal width: 2.2–2.7 mm, tapering to 0.4–0.5 mm at anal segment.

Table 1. Molecular sampling information of the present analysis.

Species	Voucher ID	Stage	Material collected location	GenBank	Remarks
Myrmeleon shalulianus sp. nov.	MJNSC1	adult	CHINA: Sichuan, Garze, Baiyu County, Gaiyu Township, 2759 m	PP453796	this paper
Myrmeleon shalulianus sp. nov.	MJNSC2	adult	CHINA: Sichuan, Liangshan, Muli County, Mairi Township, 2662 m	PP453797	this paper
Myrmeleon shalulianus sp. nov.	MJNSC3	adult	CHINA: Sichuan, Garze, Batang County, Suwalong Township, Suwalong Village, 2409 m	PP453798	this paper
Myrmeleon shalulianus sp. nov.	MJNSC4	adult	CHINA: Sichuan, Garze, Batang County, Changbo Township, Ruiwa Village, 2468 m	PP453799	this paper
Myrmeleon shalulianus sp. nov.	MJNSC5	adult	CHINA: Sichuan, Garze, Derong County, Guxue Township, Xiayong Village, 2088 m	PP453800	this paper
Myrmeleon shalulianus sp. nov.	MJNSC6	adult	CHINA: Sichuan, Garze, Derong County, Guxue Township, Xiayong Village, 2088 m	PP453801	this paper
Myrmeleon shalulianus sp. nov.	MJNYN1	adult	CHINA: Yunnan, Diqing, Shangri-la, Hutiaoxia Town, Jiangbian Village, Zanba, 2000–2100 m	PP453802	this paper
Myrmeleon trigonois	MTOCQ1	adult	CHINA: Chongqing, Wushan County, Dangyang Township, Wulipo National Natural Reserve, 1753 m	PP453803	this paper
Myrmeleon trigonois	MTOCQ2	adult	CHINA: Chongqing, Wuxi County, Lanying Township, Lanying Village, 900 m	PP453804	this paper
Myrmeleon trigonois	MTOCQ3	adult	CHINA: Chongqing, Beibei District, Mt. Jinyunshan	PP453805	this paper
Myrmeleon trigonois	MTOSC1	adult	CHINA: Sichuan, Aba, Wenchuan County, Weizhou Town, Qiangrengu, 1500–1700 m	PP453806	this paper
Myrmeleon trigonois	MTOSC2	adult	CHINA: Sichuan, Panzhihua, West District, National Nature Reserve of Cycad *Cycas panzhihuaensis*, 1508 m	PP453807	this paper
Myrmeleon trigonois	MTOSC3	adult	CHINA: Sichuan, Guangyuan, Lizhou District, Zoumaling, Longhao Aviation School, 550 m	PP453808	this paper
Myrmeleon trigonois	MTOYN1	adult	CHINA: Yunnan, Dali, Mt. Cangshan Geopark of Dali, 2200 m	PP453809	this paper
Myrmeleon tenuipennis	MTFJ1	adult	CHINA: Fujian, Longyan, Xinluo District, Mt. Tiangongshan, 650 m	PP453794	this paper
Myrmeleon tenuipennis	MTFJ2	adult	CHINA: Fujian, Longyan, Xinluo District, Mt. Tiangongshan, 650 m	PP453795	this paper
Myrmeleon inconspicuus		adult	ITALY: Emilia Romagna	JQ864060	Pantaleoni & Badano (2012)
Myrmeleon inconspicuus		adult	GREECE: Epirus	JQ864062	Pantaleoni & Badano (2012)
Myrmeleon inconspicuus		adult	ITALY: Sardinia	JQ864067	Pantaleoni & Badano (2012)
Myrmeleon punicanus		adult	ITALY: Sicily	JQ864075	Pantaleoni & Badano (2012)
Myrmeleon punicanus		adult	ITALY: Pantelleria Island	JQ864076	Pantaleoni & Badano (2012)
Myrmeleon punicanus		adult	ITALY: Pantelleria Island	Q864077	Pantaleoni & Badano (2012)
Distoleon nigricans	DNAH1 (CAU)	adult	CHINA: Anhui, Luan, Jinzhai County, Mazongling tree farm (CAU)	MW737614	Zheng et al. (2022)

Coloration predominantly pale yellow, spines dark brown to black. Head armed with 3 pairs of cephalic spines. One anterior antennal process (aap) present, basal area with one dorsal short hair and one lateral long hair (Figs 12G, H). Two posterior antennal processes (pap) present, two pap as long as aap (Figs 12G, H). Median facial hair (mfha) absent, frontal spine (fsp) merged in middle. Labral sheath (lsh) without ventral subapical process. Proboscidal sheath (prsh) short, about 0.5 length of lsh, slightly rugose laterally. Maxillary sheath (msh) smooth, extending and connecting right after prsh. Palpal sheath (pash) rugose, extending slightly over lsh (Figs 12C, D). Posterolateral facial hair (plfha) absent. Thorax mostly smooth, posterior mesothoracic callosity (pmc) small and weak. Thorax bare, without hair around pmc. Wing sheath (wsh) and basal half of leg sheaths (lesh) smooth, apical half of lesh rugose (Fig. 12D). Wsh not reaching abdominal segment 3. Fore leg sheath (lesh 1) and middle leg sheath (lesh 2) not exceeding apex of wing sheath, hind leg sheath (lesh 3) reaching abdominal segment 3. Abdomen. Eight abdominal segments visible, segments 8 and 9 fused (Fig. 12B). Abdominal tergite 1 with a few sparse short hairs. Abdominal tergites 2 to 7 with well-developed chitinous rods with posterior apex raised as spines; long hairs present laterally and sometimes between two chitinous rods on tergites 2 to 7 (Fig. 12E). Generally longer and denser hairs but fewer rods in posterior abdominal segments. Tergite 8+9 with one tiny dorsal spine, posterolateral callosity absent. Abdominal pleura 2 to 7 and 8+9 each with row of long hairs. Sternites 2 to 7 with some sparse short hairs on posterior half. Sternite 8+9 bare. Anal segment smooth, ventral callosities small and weak (Fig. 12J). Dorsal posterolateral process (dpp) small, weak, and fused, ventral posterolateral process (vpp) short and acute, with one dorsal spine and one ventral spine of similar size (Figs 12I, J).

Host. *Myrmeleon trigonois* Bao & Wang, 2006.

Bio-ecology. We observed the behavior of *Taiwanon* sp. parasitoid of two *M. trigonois* larvae. The parasitised larvae showed no abnormality from spin cocoons to pupation (we opened all the cocoons to observe the prepupa to pupa). It was not until a week after the parasitised *M. trigonois* larvae had pupated that we found the prepupa of *Taiwanon* sp. in the rearing cup. By that time, the pupae of *M. trigonois* had been consumed, their body fluids were dra-

Table 2. The genetic divergences in % among specimens analyzed in this study.

	1	2	3	4	5	6	7	8	9	10	11	12	13	14	15	16	17	18	19	20	21	22
1. *M. shalulianus* Sichuan Baiyu MJNSC1																						
2. *M. shalulianus* Sichuan Muli MJNSC2	0.3																					
3. *M. shalulianus* Sichuan Batang MJNSC3	0	0.3																				
4. *M. shalulianus* Sichuan Batang MJNSC4	0	0.3	0																			
5. *M. shalulianus* Sichuan Derong MJNSC5	0	0.3	0	0																		
6. *M. shalulianus* Sichuan Derong MJNSC6	0.2	0.5	0.2	0.2	0.2																	
7. *M. shalulianus* Yunnan Hutiaoxia MJNYN1	0	0.3	0	0	0	0.2																
8. *M. trigonois* Chongqing Wulipo MTOCQ1	3.6	4.0	3.6	3.6	3.6	3.4	3.6															
9. *M. trigonois* Chongqing Yintiaoling MTOCQ2	3.6	4.0	3.6	3.6	3.6	3.4	3.6	0														
10. *M. trigonois* Chongqing Mt.Jinyunshan MTOCQ3	3.8	4.1	3.8	3.8	3.8	3.6	3.8	0.2	0.2													
11. *M. trigonois* Sichuan Wenchuan MTOSC1	3.4	3.8	3.4	3.4	3.4	3.2	3.4	0.2	0.2	0.3												
12. *M. trigonois* Sichuan Panzhihua MTOSC2	3.4	3.8	3.4	3.4	3.4	3.2	3.4	0.2	0.2	0.3	0											
13. *M. trigonois* Yunnan Dali MTOYN1	3.6	4.0	3.6	3.6	3.6	3.4	3.6	0	0	0.2	0.2	0.2										
14. *M. trigonois* Sichuan Guangyuan MTOSC3	3.6	4.0	3.6	3.6	3.6	3.4	3.6	0	0	0.2	0.2	0.2	0									
15. *M. tenuipennis* Fujian	17.1	17.6	17.1	17.1	17.1	17.3	17.1	15.6	15.6	15.8	15.6	15.6	15.6	15.6								
16. *M. tenuipennis* Fujian	17.1	17.6	17.1	17.1	17.1	17.3	17.1	15.6	15.6	15.8	15.6	15.6	15.6	15.6	0							
17. *M. punicanus* JQ864075	17.6	18.0	17.6	17.6	17.6	17.8	17.6	17.3	17.3	17.6	17.1	17.1	17.3	17.3	15.0	15.0						
18. *M. punicanus* JQ864076	18.0	18.5	18.0	18.0	18.0	18.3	18.0	17.8	17.8	18.0	17.6	17.6	17.8	17.8	15.0	15.0	1.2					
19. *M. punicanus* JQ864077	17.8	17.8	17.8	17.8	17.8	18.0	17.8	17.6	17.6	17.8	17.3	17.3	17.6	17.6	14.5	14.5	1.4	1.2				
20. *M. inconspicuus* JQ864062	19.6	19.6	19.6	19.6	19.6	19.8	19.6	19.1	19.1	19.3	19.1	19.1	19.1	19.1	18.9	18.9	14.3	13.9	13.7			
21. *M. inconspicuus* JQ864060	19.6	19.6	19.6	19.6	19.6	19.8	19.6	19.1	19.1	19.3	19.1	19.1	19.1	19.1	18.9	18.9	14.7	14.3	14.1	0.5		
22. *M. inconspicuus* JQ864067	19.8	19.8	19.8	19.8	19.8	20.0	19.8	19.6	19.6	19.8	19.6	19.6	19.6	19.6	18.0	18.0	14.5	13.7	13.5	1.8	1.6	
23. *Distoleon nigricans*	19.8	20.3	19.8	19.8	19.8	0.2	19.8	20.3	20.3	20.5	20.0	20.0	20.3	20.3	18.0	18.0	16.0	15.4	15.6	18.7	18.4	18.2

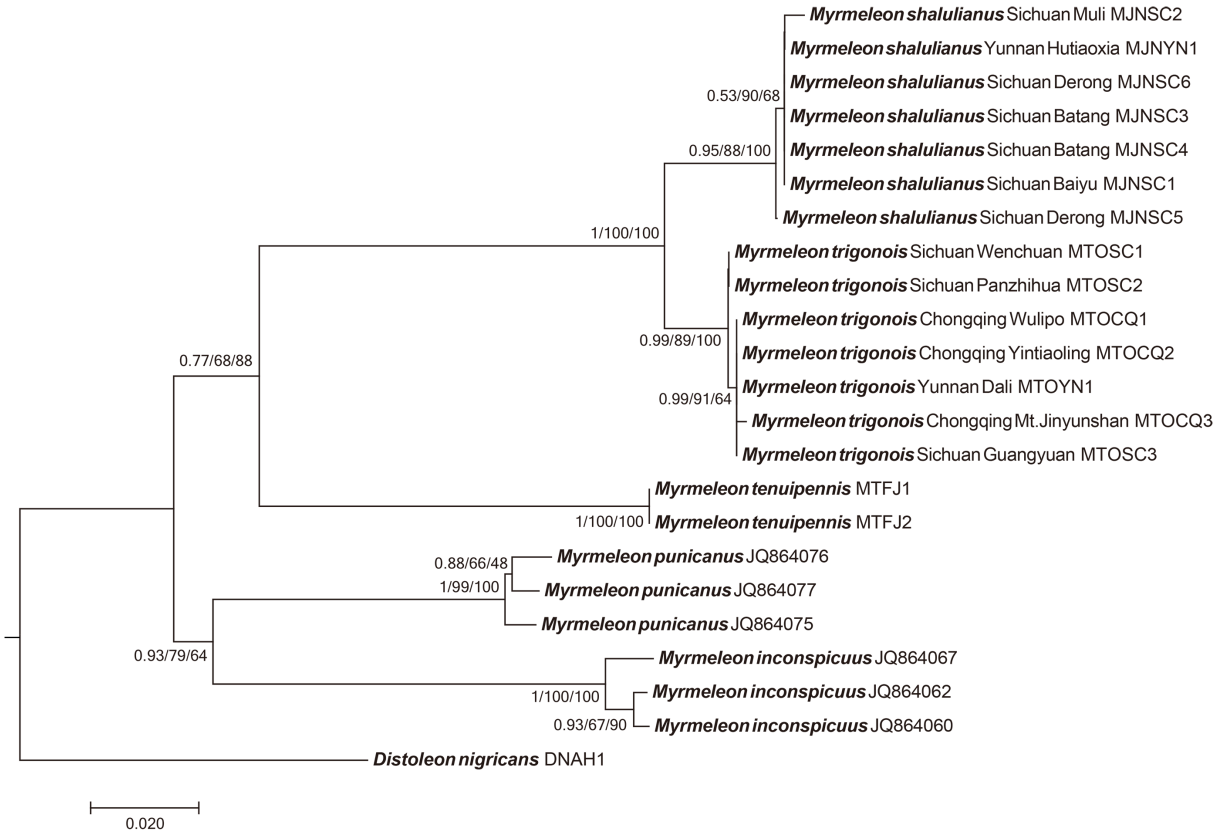

Fig. 13. Molecular phylogeny of selected species of Myrmeleontidae based on COI barcoding sequence data. Tree topologies are identical among the Bayesian inference, Maximum likelihood, and Neighbour-joining analyses. Nodal supports include the posterior probabilities of Bayesian inference/ bootstrap values of Maximum likelihood analysis/bootstrap values of Neighbour-joining analysis.

ined, but their body surfaces were left entirely intact. We assume that larvae of *Taiwanon* sp. are endoparasitic and may be able to diapause for the period of host larvae until the host cocoons and pupates before rapidly consuming the host and pupating, allowing *Taiwanon* sp. to use the cocoons of *M. trigonois* to protect itself during its pupal stage. Considering that the two specimens of *Taiwanon* sp. are both females, we tentatively treat this species as an undetermined one.

Remarks. The present species is similar to *Taiwanon phormae* Evenhuis, 2018. Without comparing the male genitalia, we are not sure whether it is the same species or not. To stay on the safe side, we prefer not to name a new species based on the available female specimens.

Variation in cell cua was observed. On the same specimen, cell cua was closed on the left wing and opened on the right wing (Fig. 11A). We described cell cua as open, based on the most common status of two observed specimens.

In the key to world genera of Villoestrini by Evenhuis (2018), vein R4+5 curved downward or upward was used to discriminate *Taiwanon* and *Oestranthrax*. All R4+5 in Evenhuis (2018) refer to R4 instead.

Molecular identification

The COI interspecific genetic divergence among the five examined species of *Myrmeleon* ranges from 0.034 to 0.200 (Table 2). The interspecific genetic divergence between *M. shalulianus* sp. nov. and *M. trigonois* ranges from 0.032 to 0.041. The intraspecific genetic divergence within each *M. shalulianus* sp. nov. and *M. trigonois* ranges from 0.000 to 0.003. None of the intraspecific genetic divergences within the other three *Myrmeleon* species in the analysis ranges higher than 0.018. Thus, it can be shown that there is a significant genetic distance gap between *M. shalulianus* sp. nov. and *M. trigonois*. In all trees generated by the three phylogenetic analyses (Fig. 14), the topologies are identical. It is important to note that these results are only used to distinguish species by COI barcodes rather than infer their phylogenetic relationship.

Discussion

In Southwest China, especially the Hengduan mountain system, many environmental types are highly differentiated by altitude, latitude, and regional microclimatic variation (Zhu & Tan 2023). The Shaluli mountain range is the widest mountain range in the Hengduan mountain system, containing glacial relicts at high altitudes as well as mid-elevation dry and hot river valleys of the Jinshajiang River. This situation represents a natural barrier to species dispersal, leading to species isolation and divergence (Zhou et al. 2013). *Myrmeleon shalulianus* sp. nov. is only restricted to the mid-elevation dry-hot river valleys of the Jinshajiang River from the Shaluli mountain range. On the other hand, *M. trigonois* is widespread in low- to

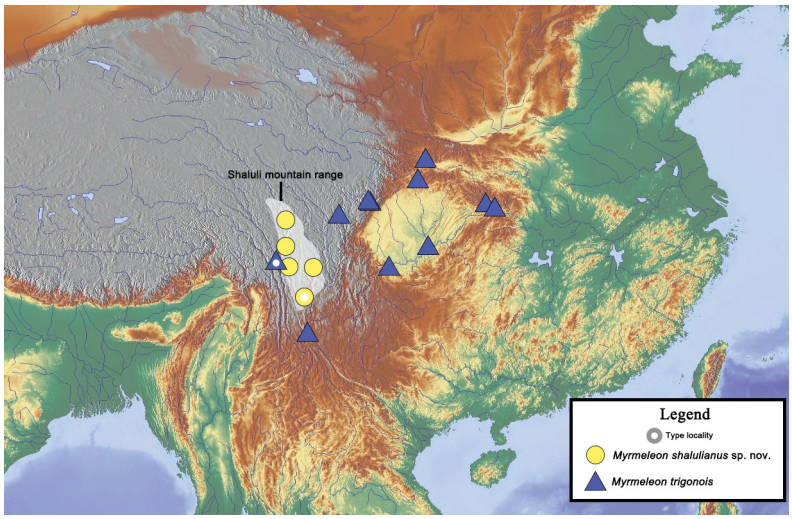

Fig. 14. Distribution map of *Myrmeleon shalulianus* Zheng & Liu sp. nov. and *M. trigonois* Bao & Wang, 2006.

mid-elevations of humid, densely vegetated mountains from the Yunling mountain range to the Wushan mountain range. It is worth noting that some distributional areas of *M. trigonois* (e.g., Dali and Deqen from Yunnan) are near the range of *M. shalulianus* sp. nov., but none of these localities are from the Shaluli mountain range. Thus, these species are not sympatric.

Compared to some clades of Dendroleontinae with DNA barcoding analyses of genetic divergence (i.e., *Layahima* Navás, 1912, *Nepsalus* Navás, 1914, and *Paralayahima* Zheng, Badano & Liu, 2023, with at least 0.06) (Zheng et al. 2022, 2023), the genetic divergence between *M. shalulianus* sp. nov. and *M. trigonois* is relatively small (ranges from 0.032 to 0.041). However, different clades present different evolutionary histories, and species should be distinguished based on morphology, distribution, and the scales of genetic divergence within the same major clade. Morphologically, they exhibit stable and significant differences (see Comparative notes for *M. shalulianus* sp. nov.). Although *M. trigonois* is widespread in Southwest China, our results show that the intraspecific genetic distances of *M. trigonois* from many distant localities are also extremely small (range from 0.000 to 0.003), similar to *M. shalulianus* sp. nov. (range from 0.000 to 0.003) (Table 2). Besides, even though some populations of *M. trigonois* are distributed in the areas near those of *M. shalulianus* sp. nov., their genetic divergence is not close. Such relatively small genetic divergence between related *Myrmeleon* species may be due to the late formation of the young Hengduan mountain system (formed during the Late Miocene to Pliocene) (Favre et al. 2015, Ding et al. 2020, Spicer et al. 2021), where some of the related species might have just diverged with the geographical isolation.

Acknowledgements

We sincerely thank Dr. Di Li, Mr. Hao Xun, Mr. Haolin Gan, and Mr. Yuezheng Tu for collecting the new species *M. shalulianus* sp. nov. We are grateful to Dr. Jishen Wang, Ms. Jialing Li, Ms. Lu Yue, Ms. Lulan Jie, Ms. Qiaoqiao Liu and Mr. Wenkai Kou for collecting the specimens of *M. trigonios*. We would also like to appreciate Ms. Xiaohong Ye, Mr. Zhongxia Zheng, Mr. Baozhi Ge, Dr. Zhisheng Zhang and Dr. Hao Xu as they helped the first author in collecting the larvae of *M. shalulianus* sp. nov. and *M. trigonios* in the field. We thank Michael Zelun Lee for assisting us in obtaining specimens of *M. shalulianus* sp. nov. We are also grateful to Ms. Haoyue Zhou for her assistance in taking photos of the adult specimen and the pupal exuviae of the bee fly, and Dr. Neal Evenhuis for sharing bee fly references. We also sincerely thank Dr. Di Li and Mr. Wenkai Kou for sharing the photos of pit-form traps of larvae and their habitat with us. We thank Ms. Yan Lai for providing technical help with molecular analysis. Finally, we are grateful to the editor, Dr. Petr Kočárek (University of Ostrava, Czech Republic), and two anonymous reviewers for their edits and comments on the manuscript. This research was supported by the National Natural Science Foundation of China (No. 31970435, 32370484), the National Animal Collection Resource Center, China, the Fund on survey of spiders and insects from Yintiaoling Nature Reserve, and the Biodiversity Survey and Assessment Project of the Ministry of Ecology and Environment, China (2019HJ2096001006).

References

ÁBRAHÁM L. 2017: *Myrmeleon wangxinlii* sp. n. (Neuroptera: Myrmeleontidae) from Sichuan, China. *Acta Entomologica Silesiana* **25**: 1–9.

ASPÖCK U. & ASPÖCK H. 2008: Phylogenetic relevance of the genital sclerites of Neuropterida (Insecta: Holometabola). *Systematic Entomology* **33**: 97–127.

BADANO D., ACEVEDO F., PANTALEONI R. A. & MONSERRAT V. J. 2016: *Myrmeleon almohadarum* sp. nov., from Spain and North Africa, with description of the larva (Neuroptera Myrmeleontidae). *Zootaxa* **4196**: 210–220.

BADANO D., ASPÖCK U., ASPÖCK H. & CERRETTI P. 2017a: Phylogeny of Myrmeleontiformia based on larval morphology (Neuropterida: Neuroptera). *Systematic Entomology* **42**: 94–117.

BADANO D., ASPÖCK H. & ASPÖCK U. 2017b: Taxonomy and phylogeny of the genera *Gymnocnemia* Schneider, 1845, and *Megistopus* Rambur, 1842, with remarks on the systematization of the tribe Nemoleontini (Neuroptera, Myrmeleontidae). *Deutsche Entomologische Zeitschrift* **64**: 43–60.

BADANO D., ASPÖCK H., ASPÖCK U. & HARING E. 2017c: Eyes in the dark … Shedding light on the antlion phylogeny and the enigmatic genus *Pseudimares* Kimmins (Neuropterida: Neuroptera: Myrmeleontidae). *Arthropod Systematics and Phylogeny* **75**: 535–554.

BADANO D. & PANTALEONI R. A. 2014: The larvae of European Myrmeleontidae (Neuroptera). *Zootaxa* **3762**: 1–71.

BAO R. & WANG X. L. 2006: Two new species of *Myrmeleon* Linnaeus, 1767 (Neuroptera: Myrmeleontidae) from China, with a key to Chinese species. *Proceedings of the Entomological Society of Washington* **108**: 125–130.

BREITKREUZ L. C. V., WINTERTON S. L. & ENGEL M. S. 2017: Wing tracheation in Chrysopidae and other Neuropterida (Insecta): a resolution of the confusion about vein fusion. *American Museum Novitates* **3890**: 1–44.

DEVETAK D., KLOKOČOVNIK V., LIPOVŠEK S., BOCK E. & LEITINGER G. 2013: Larval morphology of the antlion *Myrmecaelurus trigrammus* (Pallas, 1771) (Neuroptera, Myrmeleontidae), with notes on larval biology. *Zootaxa* **3641**: 491–500.

DING W. N., REE R. H., SPICER R. A. & XING Y. W. 2020: Ancient orogenic and monsoon-driven assembly of the world's richest temperate alpine flora. *Science* **369**: 578–581.

EVENHUIS N. L. 2018: A new genus and species of Villoestrini Hull (Diptera: Bombyliidae) from the Oriental Region parasitic on ant lions (Neuroptera: Myrmeleontidae), with key to genera in the tribe. *Bishop Museum Occasional Papers* **124**: 1–10.

FAVRE A., PÄCKERT M., PAULS S. U., JÄHNIG S. C., UHL D., MICHALAK I. & MUELLNER-RIEHL A. N. 2015: The role of the uplift of the Qinghai-Tibetan Plateau for the evolution of Tibetan biotas. *Biological Reviews* **90**: 236–253.

KIMURA M. 1980: A simple method for estimating evolutionary rates of base substitutions through comparative studies of nucleotide sequences. *Journal of Molecular Evolution* **16**: 111–120.

KLOKOČOVNIK V. & DEVETAK D. 2022: Efficiency of antlion trap design and larval behavior in capture success. *Behavioral Ecology* **33**: 184–189.

LAI Y., LIU Y. H. & LIU X. Y. 2021: Elevational diversity patterns of Green Lacewings (Neuroptera: Chrysopidae) uncovered with DNA barcoding in a biodiversity hotspot of southwest China. *Frontiers in Ecology and Evolution* **9 (778686)**: 1–14.

LATREILLE P. A. 1810: *Considérations générales sur l'ordre naturel des animaux composant les classes des Crustacés, des Arachnides, et des Insectes; avec un tableau méthodique de leurs genres, disposés en familles*. Schoell, Paris, 444 pp.

LINNAEUS C. 1767: *Systema naturae per regna tria naturae secundum classes, ordines, genera, species, cum characteribus, differentiis, synonymis, locis. Editio duodecima, reformata* [= 12th edition, revised]. *Tom. I, Pars II* [= Vol. 1, pt. 2]. Laurentii Salvii, Holmiae, pp. 533–1327.

MACHADO R. J. P., GILLUNG J. P., WINTERTON S. L., GARZÓN-ORDUÑA I. J., LEMMON A. R., LEMMON E. M. & OSWALD J. D. 2019: Owlflies are derived antlions: anchored phylogenomics supports a new phylogeny and classification of Myrmeleontidae (Neuroptera). *Systematic Entomology* **44**: 418–450.

MACHADO R. J. P. & OSWALD J. D. 2020: Morphological phylogeny and taxonomic revision of the former antlion subtribe Periclystina (Neuroptera: Myrmeleontidae: Dendroleontinae). *Zootaxa* **4796**: 1–322.

MANSELL M. W. 1999: Evolution and success of antlions (Neuropterida: Neuroptera: Myrmeleontidae). *Stapfia* **60**: 49–58.

MICHEL B. & AKOUDJIN M. 2023: Description of three new species of *Myrmeleon* Linnaeus, 1767 from West Africa (Neuroptera: Myrmeleontidae). *Zootaxa* **5231**: 414–426.

MICHEL B., CLAMENS A. L., BÉTHOUX O., KERGOAT G. J. & CONDAMINE F. L. 2017: A first higher-level time-calibrated phylogeny of antlions (Neuroptera: Myrmeleontidae). *Molecular Phylogenetics and Evolution* **107**: 103–116.

MILLER M. A., PFEIFFER W. & SCHWARTZ T. 2010: *Creating the CIPRES Science Gateway for inference of large phylogenetic trees. Gateway Computing Environments Workshop (GCE)*. New Orleans, LA, 8 pp.

NARTSHUK E. P., KRIVOKHATSKY V. A. & EVENHUIS N. L. 2019: First record of a bee fly (Diptera: Bombyliidae) parasitic on antlions (Myrmeleontidae) in Russia. *Russian Entomological Journal* **28**: 189–191.

NGUYEN L. T., SCHMIDT H. A., VON HAESELER A. & MINH B. Q. 2015: IQ-TREE: a fast and effective stochastic algorithm for estimating maximum likelihood phylogenies. *Molecular Biology and Evolution* **32**: 268–274.

OSWALD J. D. 2023: *Neuropterida Species of the World*. Lacewing Digital Library, Research Publication No. 1. http://lacewing.tamu.edu/SpeciesCatalog/Main. Last accessed 5 December 2022.

PANTALEONI R. A. & BADANO D. 2012: *Myrmeleon punicanus* n. sp., a new pit-building antlion (Neuroptera Myrmeleontidae) from Sicily and Pantelleria. *Bulletin of Insectology* **65**: 139–148.

PARK D. S., SUH S. J., OH H. W. & HEBERT P. D. N. 2010: Recovery of the mitochondrial COI barcode region in diverse Hexapoda through tRNA-based primers. *BMC Genomics* **11 (423)**: 1–7.

SPICER R. A., SU T., VALDES P. J., FARNSWORTH A., WU F. X., SHI G. L., SPICER T. E. V. & ZHOU Z. K. 2021: Why 'the uplift of the Tibetan Plateau' is a myth. *National Science Review* **8 (nwaa091)**: 1–19.

STANGE L. A. 2004: A systematic catalog, bibliography and classification of the world antlions (Insecta: Neuroptera: Myrmeleontidae). *Memoirs of the American Entomological Institute* **74**: 1–565.

TAMURA K., STECHER G., PETERSON D., FILIPSKI A. & KUMAR S. 2013: MEGA6: Molecular Evolutionary Genetics Analysis Version 6.0. *Molecular Biology and Evolution* **30**: 2725–2729.

WANG X. L., ZHAN Q. B. & WANG A. Q. 2018: *Fauna Sinica Insecta Vol. 68 Neuroptera Myrmeleontoidea*. Science Press, Beijing, 285 pp (in Chinese).

YANG D., LIU X. Y. & YANG X. K. 2018: *Species Catalogue of China. Vol. 2, Animals, Insecta (II), Neuropterida*. Science Press, Beijing, 112 pp (in Chinese).

ZHENG Y. C., BADANO D. & LIU X. Y. 2023: Systematic revision, molecular phylogeny and biogeography of the antlion tribe Acanthoplectrini (Neuroptera: Myrmeleontidae: Dendroleontinae), with emphasis on the Oriental lineage. *Systematic Entomology* **48**: 40–68.

ZHENG Y. C., HAYASHI F., PRICE B. W. & LIU X. Y. 2022: Unveiling the evolutionary history of a puzzling antlion genus *Gatzara* Navás (Neuroptera: Myrmeleontidae: Dendroleontinae) based on systematic revision, molecular phylogenetics, and biogeographic inference. *Insect Systematics and Diversity* **6 (3)**: 1–22.

ZHOU Z., HONG D. Y., NIU Y., LI G. D., NIE Z. L., WEN J. & SUN H. 2013: Phylogenetic and biogeographic analyses of the Sino-Himalayan endemic genus *Cyananthus* (Campanulaceae) and implications for the evolution of its sexual system. *Molecular Phylogenetics and Evolution* **68**: 482–497.

ZHU H. & TAN Y. 2022: Flora and vegetation of Yunnan, Southwestern China: Diversity, origin and evolution. *Diversity* **14 (5) (340)**: 1–18.